Supplementary Information

Indium(III) complexes with Schiff base-derived polydentate ligands: chemotherapeutic, radiochemotherapeutic, and radiosensitizer potentials against breast tumor cells

Andrea R. Aguirre[a], Gabrieli L. Parrilha[a], Gabriel Henrique C. Braga[a], Raquel G. Dos Santos*[b], Heloisa Beraldo*[a].

[a] Departamento de Química, Universidade Federal de Minas Gerais, 31.270-901, Belo Horizonte, Brazil.

[b] Centro de Desenvolvimento da Tecnologia Nuclear, 31.270-901, Belo Horizonte, Brazil.

Table of contents

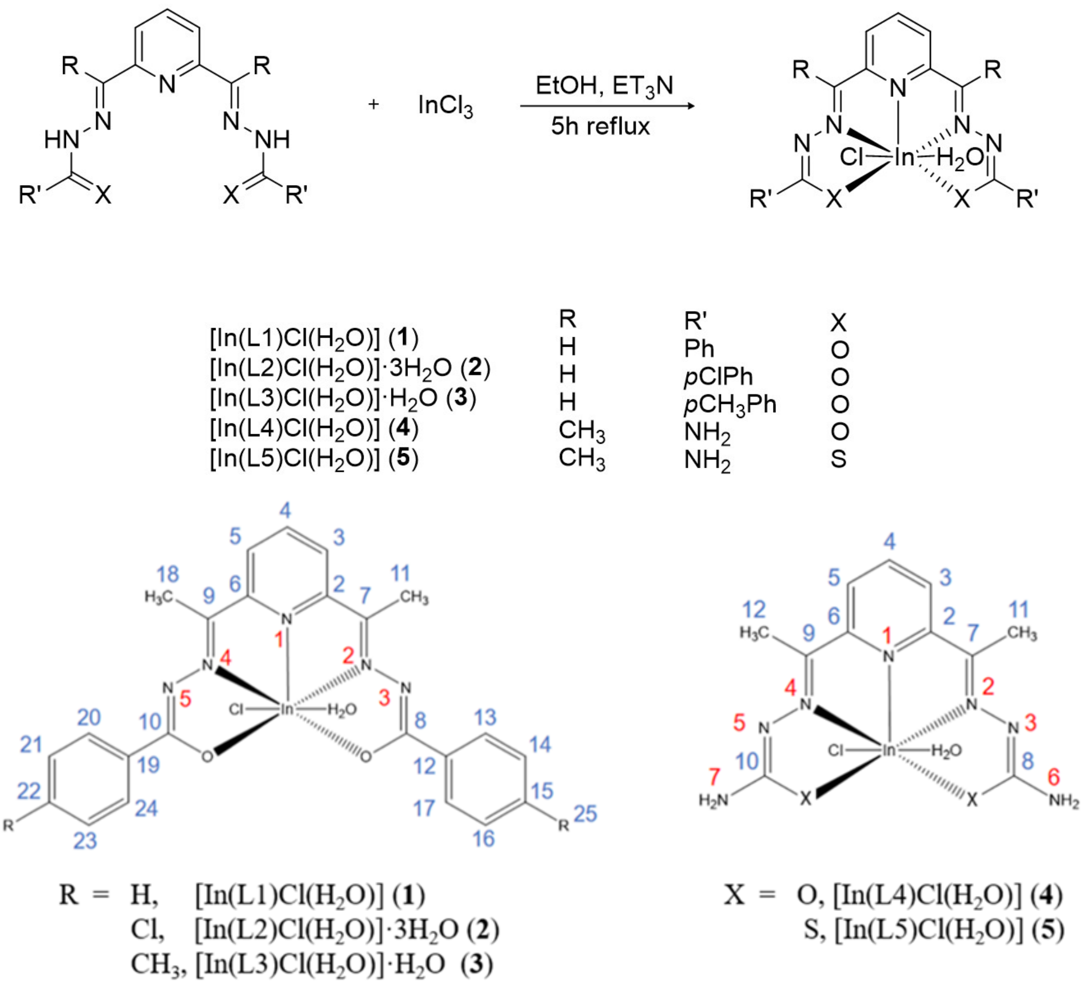

Scheme S1. General scheme for the synthesis of indium(III) complexes **1-5** and atom numbering for complexes **1-5**

Thermogravimetry

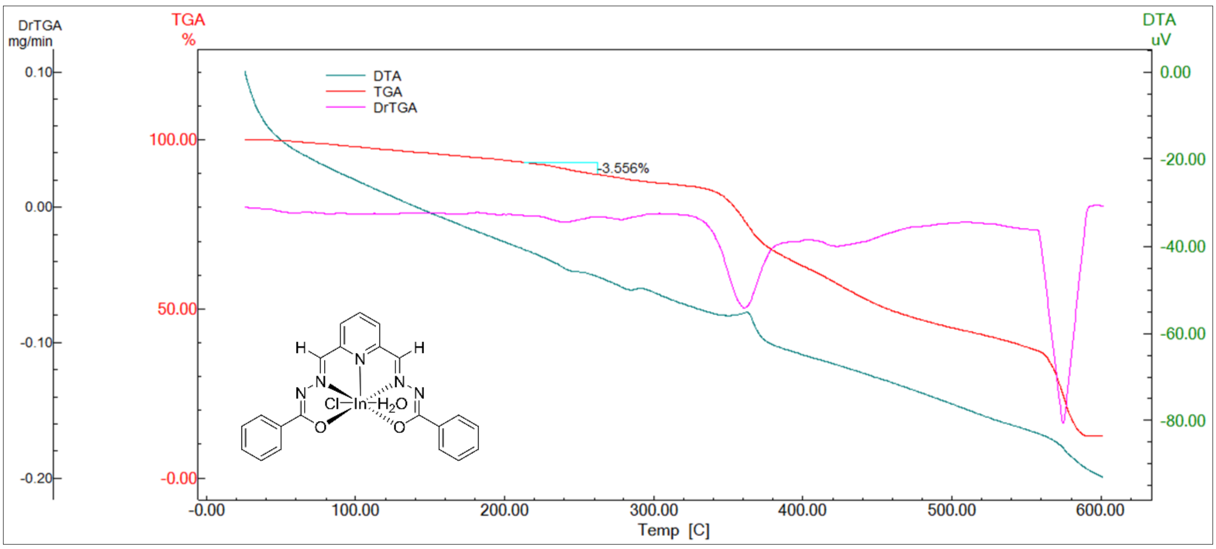

Figure S1. Thermogravimetry of complex [In(L1)Cl(H_2O)] (**1**)

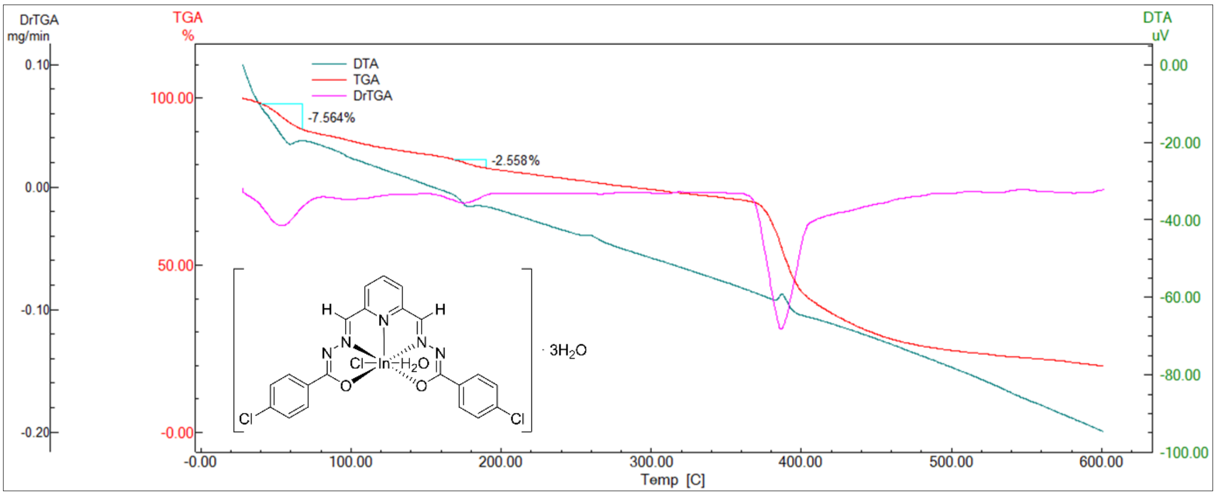

Figure S2. Thermogravimetry of complex [In(L2)Cl(H_2O)]·3H_2O (**2**)

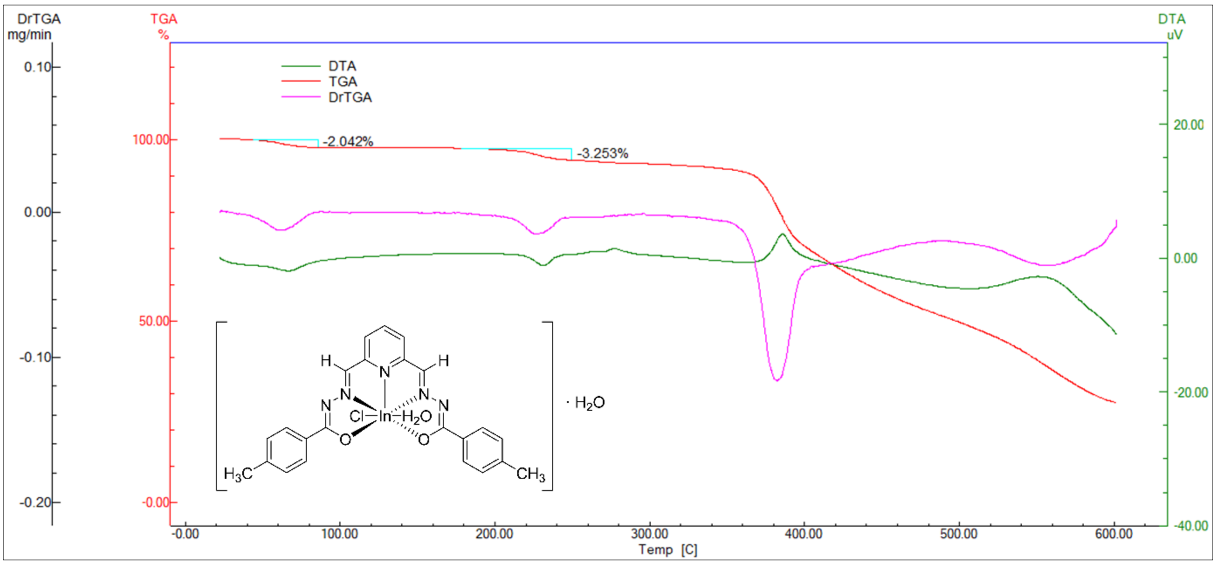

Figure S3. Thermogravimetry of complex [In(L3)Cl(H_2O)]·H_2O (**3**)

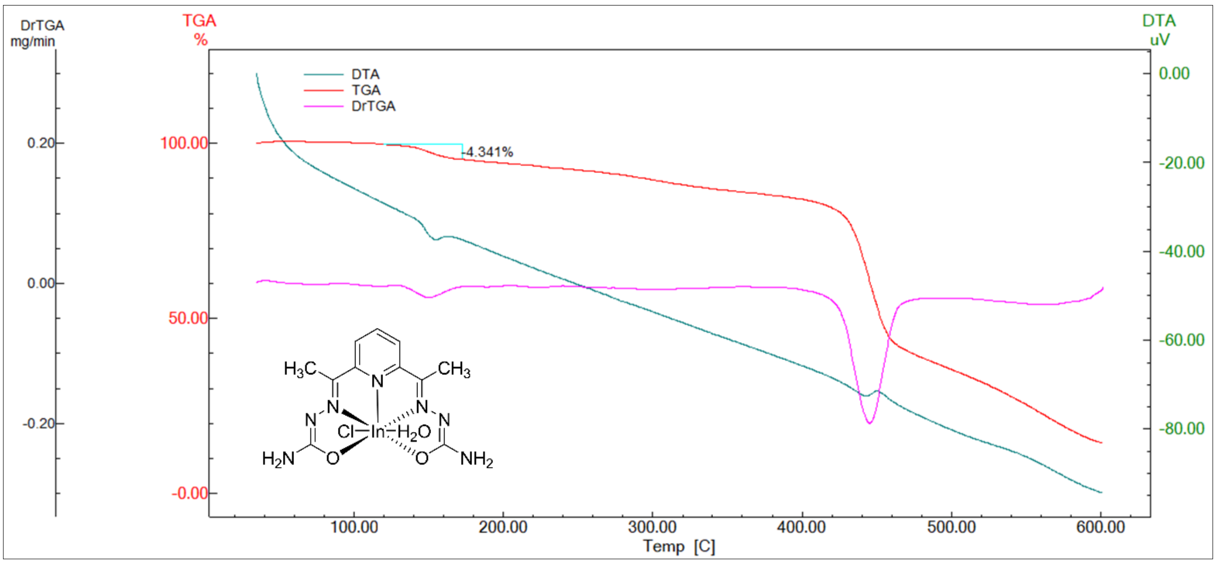

Figure S4. Thermogravimetry of complex [In(L4)Cl(H_2O)] (**4**)

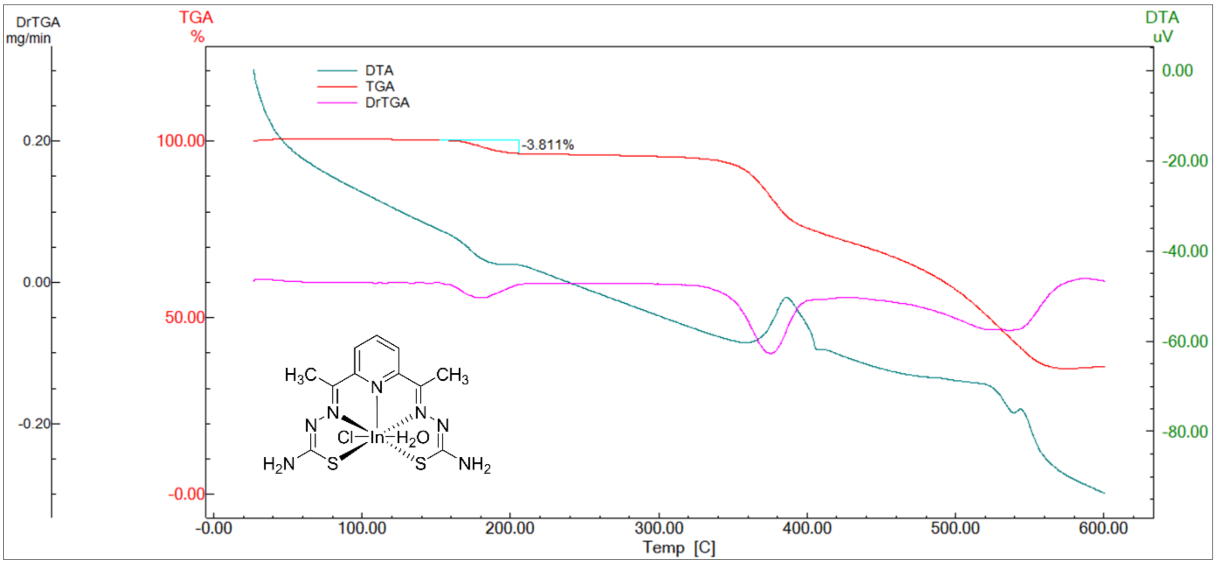

Figure S5. Thermogravimetry of complex [In(L5)Cl(H_2O)] (**5**)

Infrared Spectra

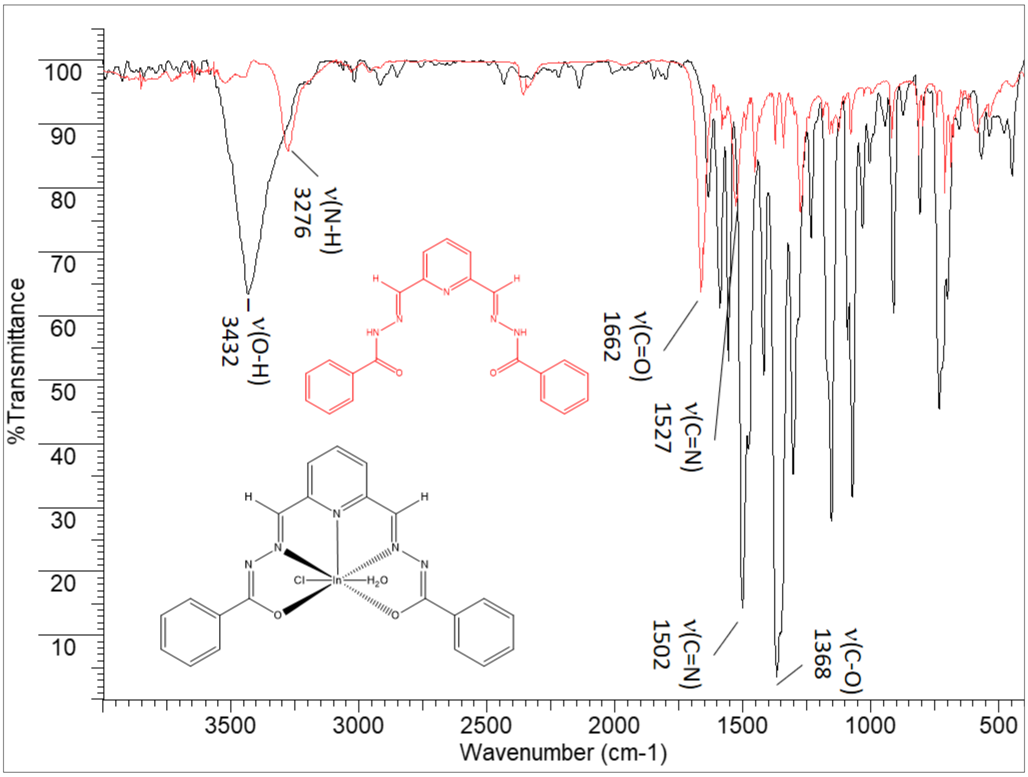

Figure S6. Infrared spectra of H_2L1 and complex [In(L1)Cl(H_2O)] (**1**)

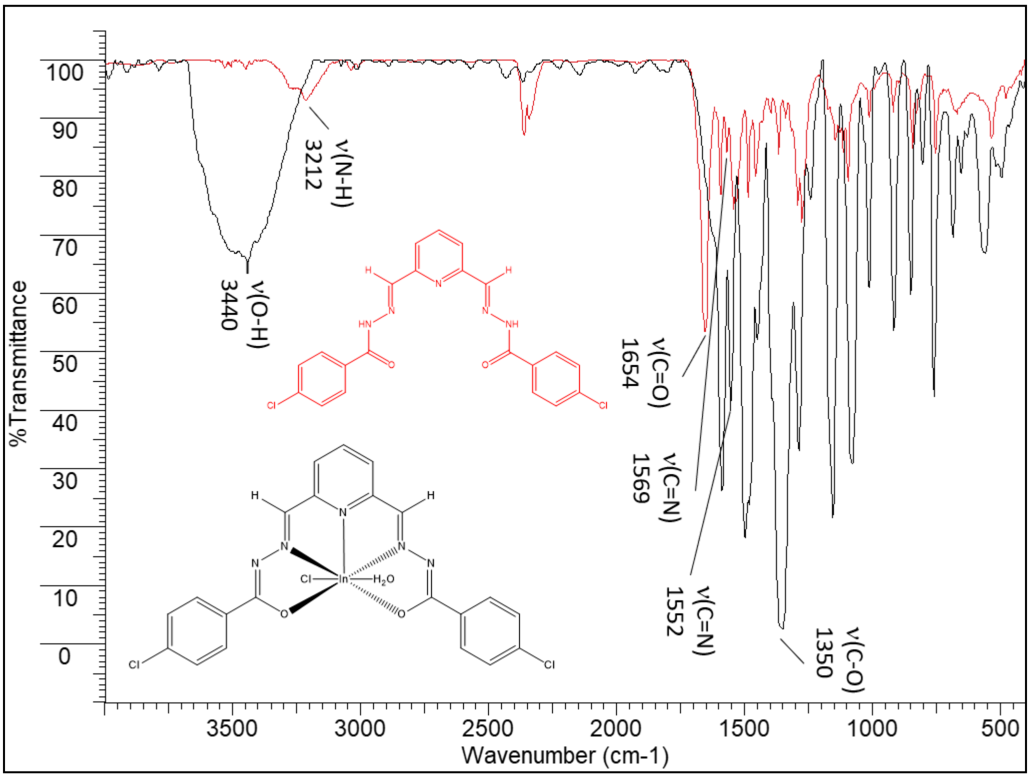

Figure S7. Infrared spectra of H_2L2 and complex $[In(L2)Cl(H_2O)]\cdot 3H_2O$ (**2**)

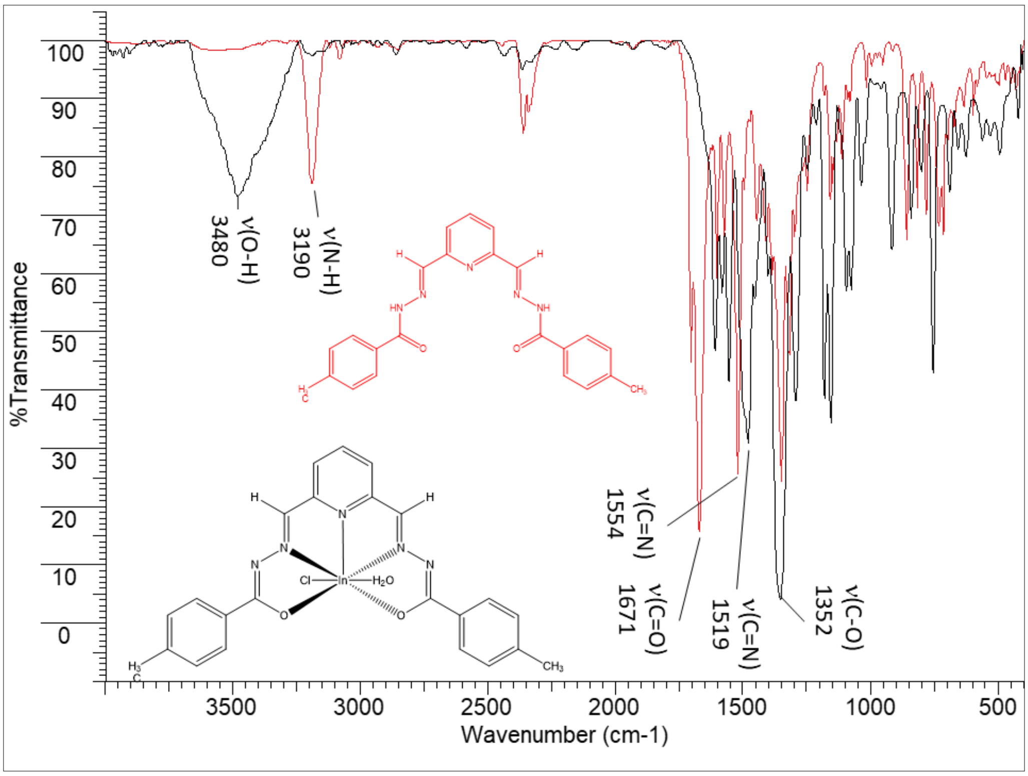

Figure S8. Infrared spectra of H_2L3 and complex $[In(L3)Cl(H_2O)]\cdot H_2O$ (**3**)

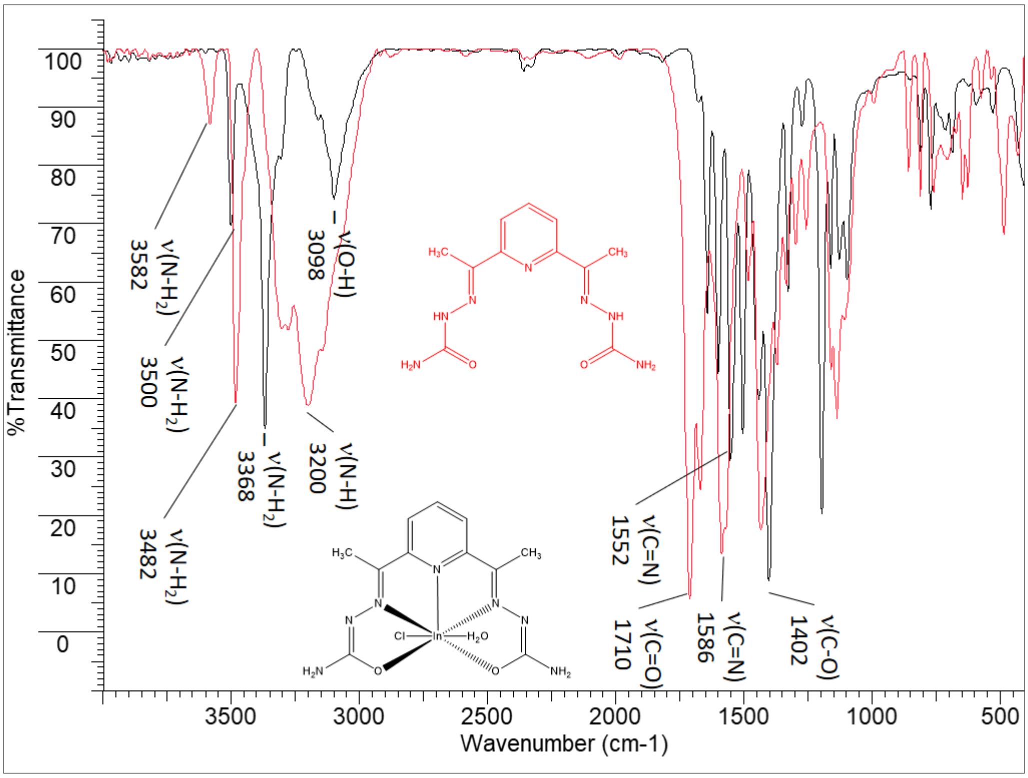

Figure S9. Infrared spectra of H_2L4 and complex [In(L4)Cl(H$_2$O)] (**4**)

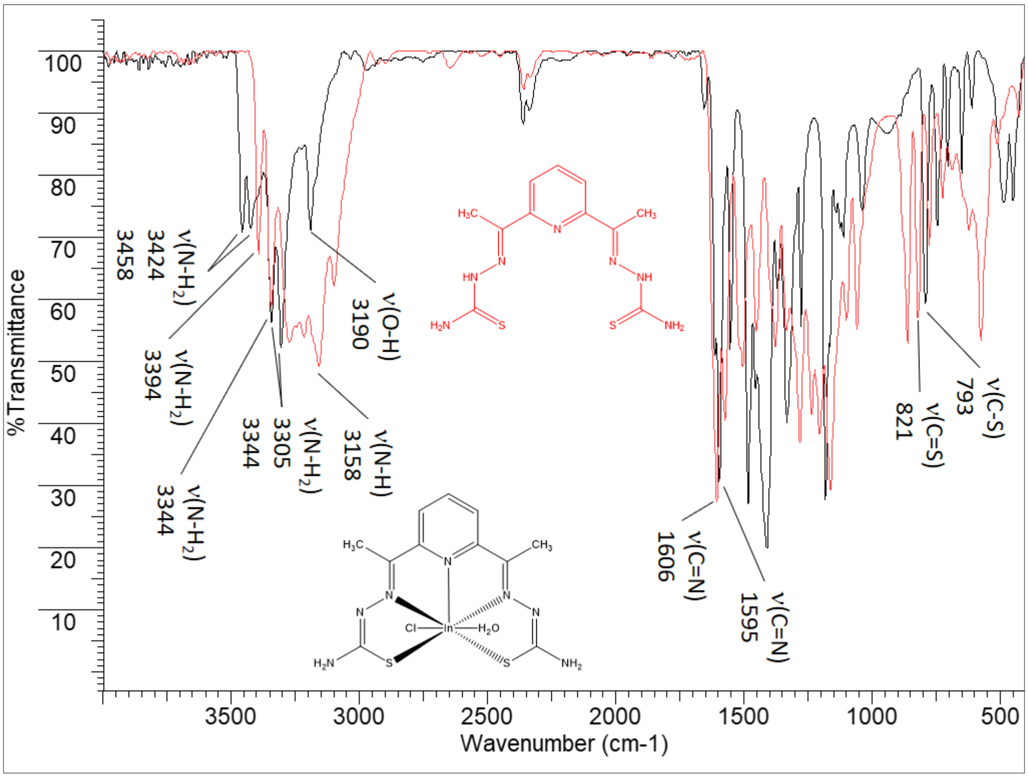

Figure S10. Infrared spectra of H_2L5 and complex [In(L5)Cl(H$_2$O)] (**5**)

NMR Spectra

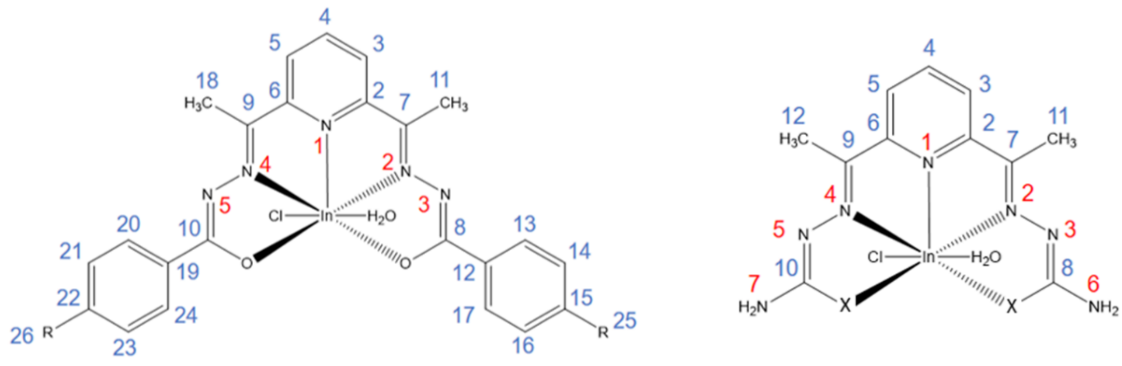

R = H, $[In(L1)Cl(H_2O)]$ (**1**)
Cl, $[In(L2)Cl(H_2O)]\cdot 3H_2O$ (**2**)
CH_3, $[In(L3)Cl(H_2O)]\cdot H_2O$ (**3**)

X = O, $[In(L4)Cl(H_2O)]$ (**4**)
S, $[In(L5)Cl(H_2O)]$ (**5**)

Figure S11. Structural representation of indium(III) complexes **1-5** with atom numbering

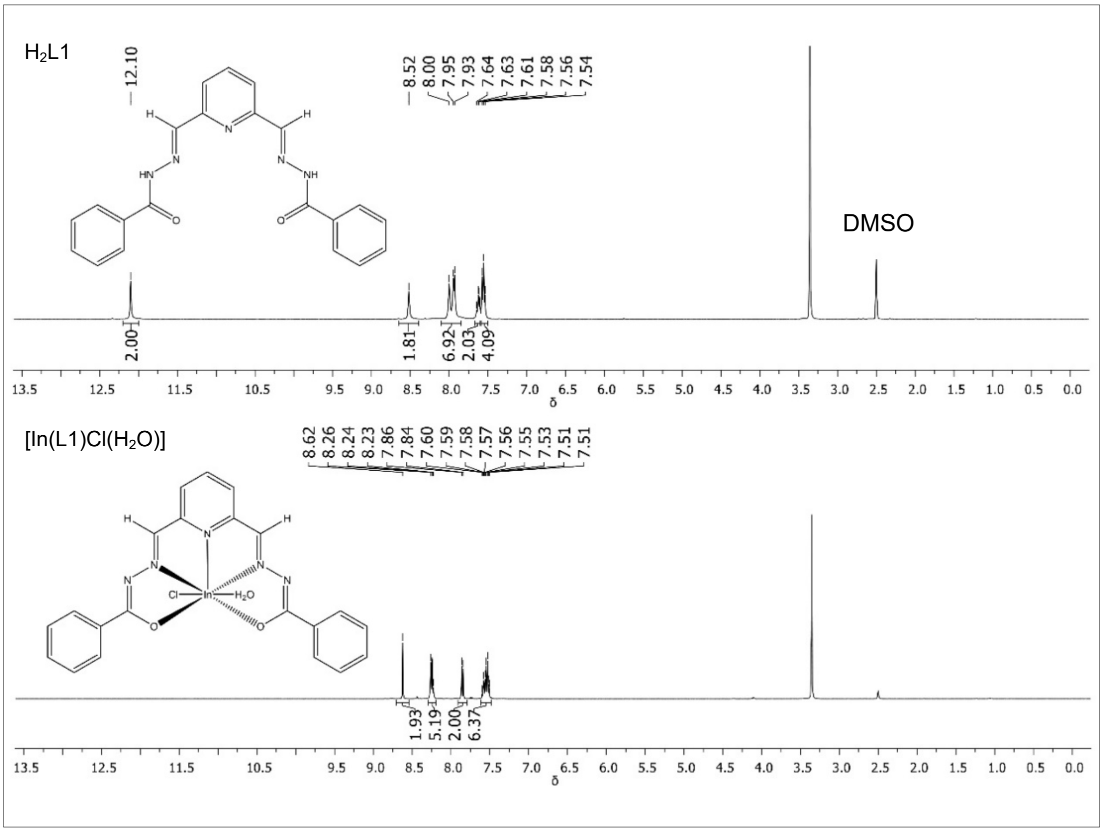

Figure S12. ^{1}H NMR spectra of H_2L1 and complex $[In(L1)Cl(H_2O)]$ (**1**)

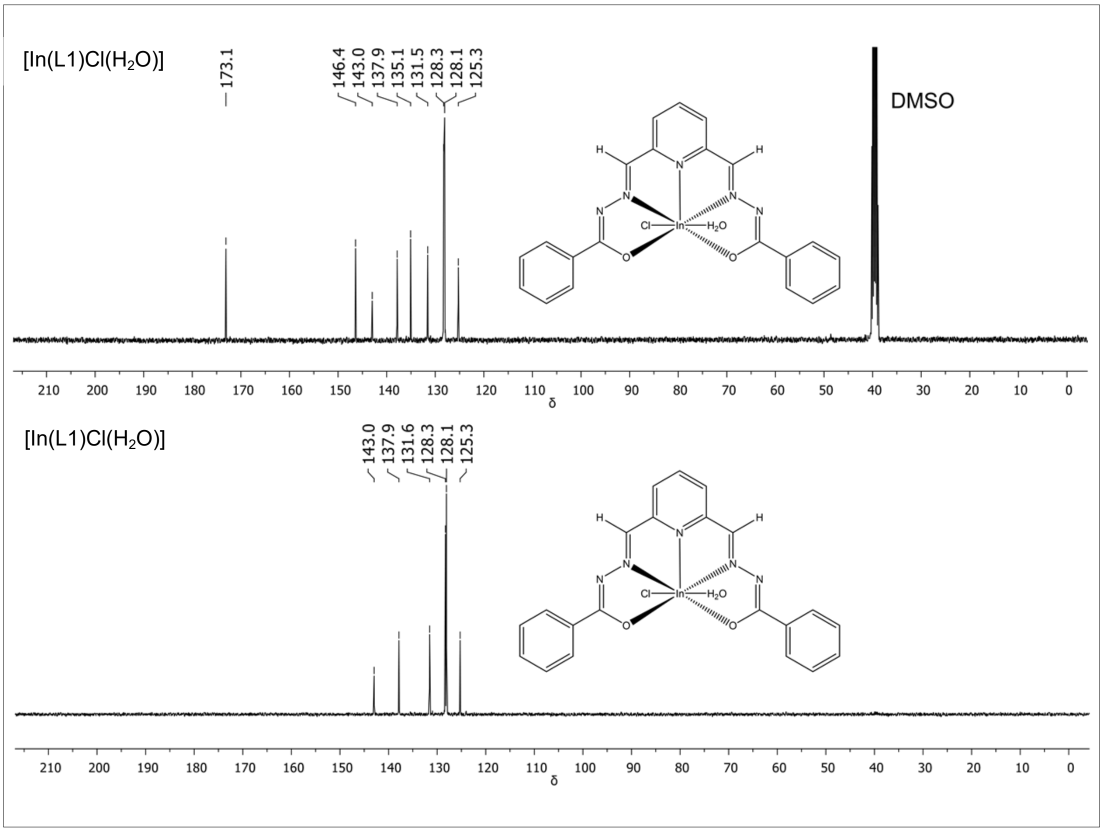

Figure S13. $^{13}C\{^1H\}$and DEPT-135 NMR spectra of complex [In(L1)Cl(H_2O)] (**1**)

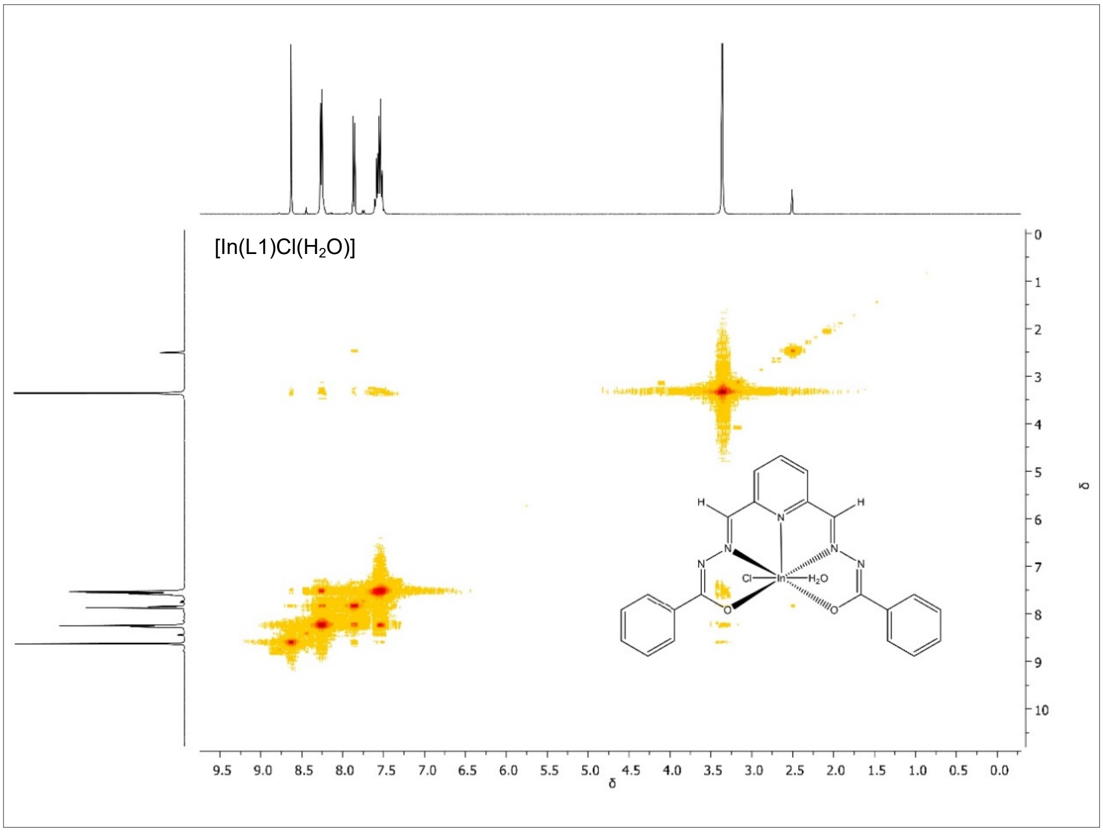

Figure S14. COSY NMR spectrum of complex [In(L1)Cl(H_2O)] (**1**)

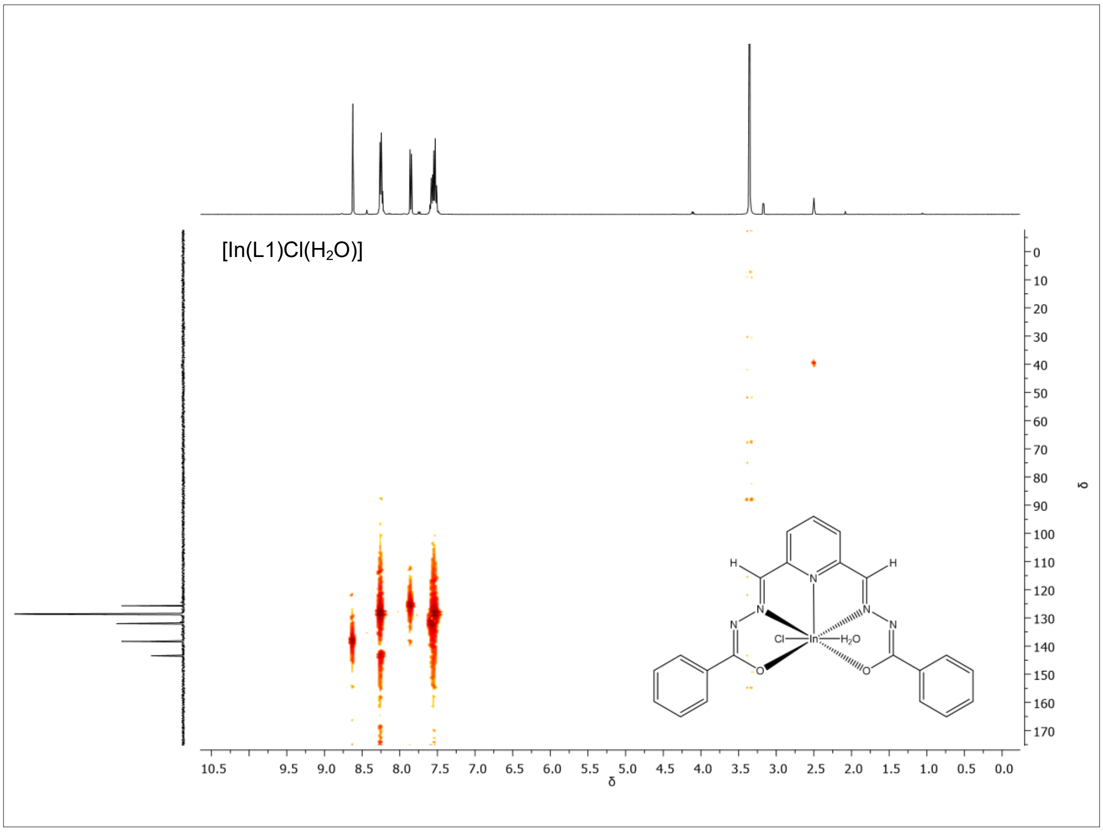

Figure S15. HMQC NMR spectrum of complex [In(L1)Cl(H_2O)] (**1**)

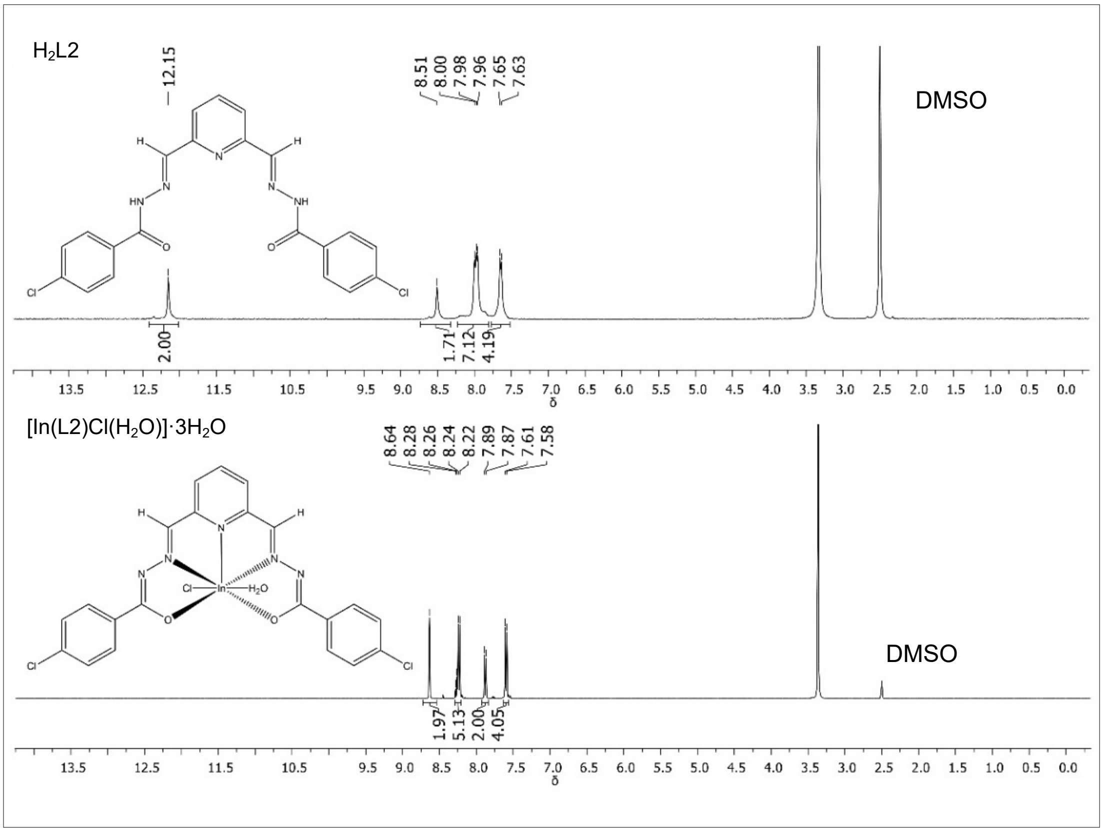

Figure S16. ¹H NMR spectra of H_2L2 and complex [In(L2)Cl(H_2O)]·$3H_2O$ (**2**)

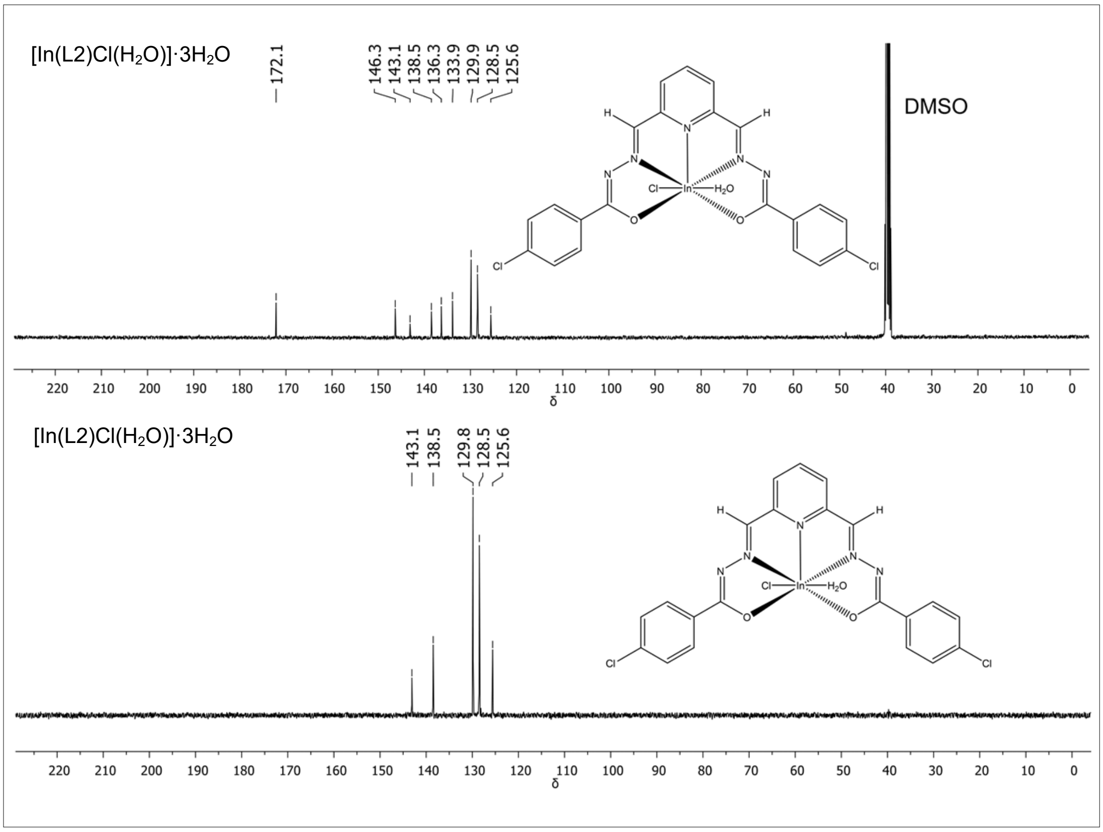

Figure S17. $^{13}C\{^1H\}$and DEPT-135 NMR spectra of complex [In(L2)Cl(H_2O)]·3H_2O (**2**)

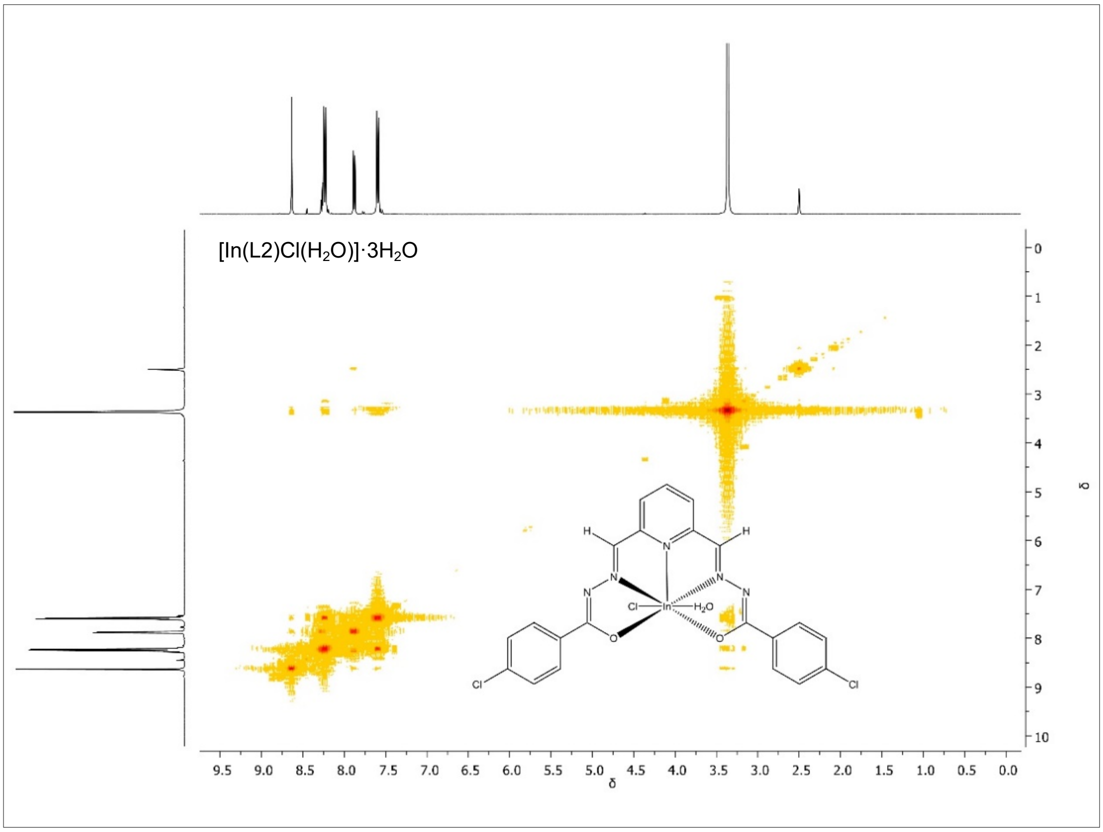

Figure S18. COSY NMR spectrum of complex [In(L2)Cl(H_2O)]·3H_2O (**2**)

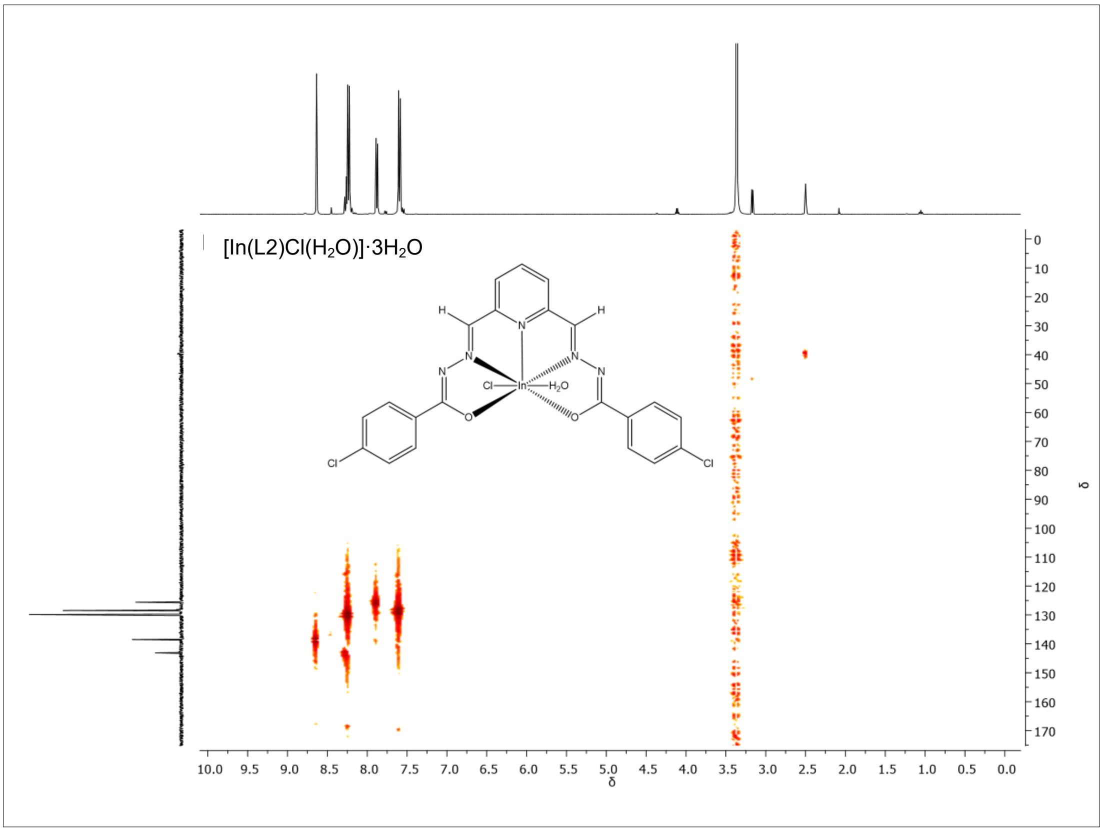

Figure S19. HMQC NMR spectrum of complex [In(L2)Cl(H_2O)]·3H_2O (**2**)

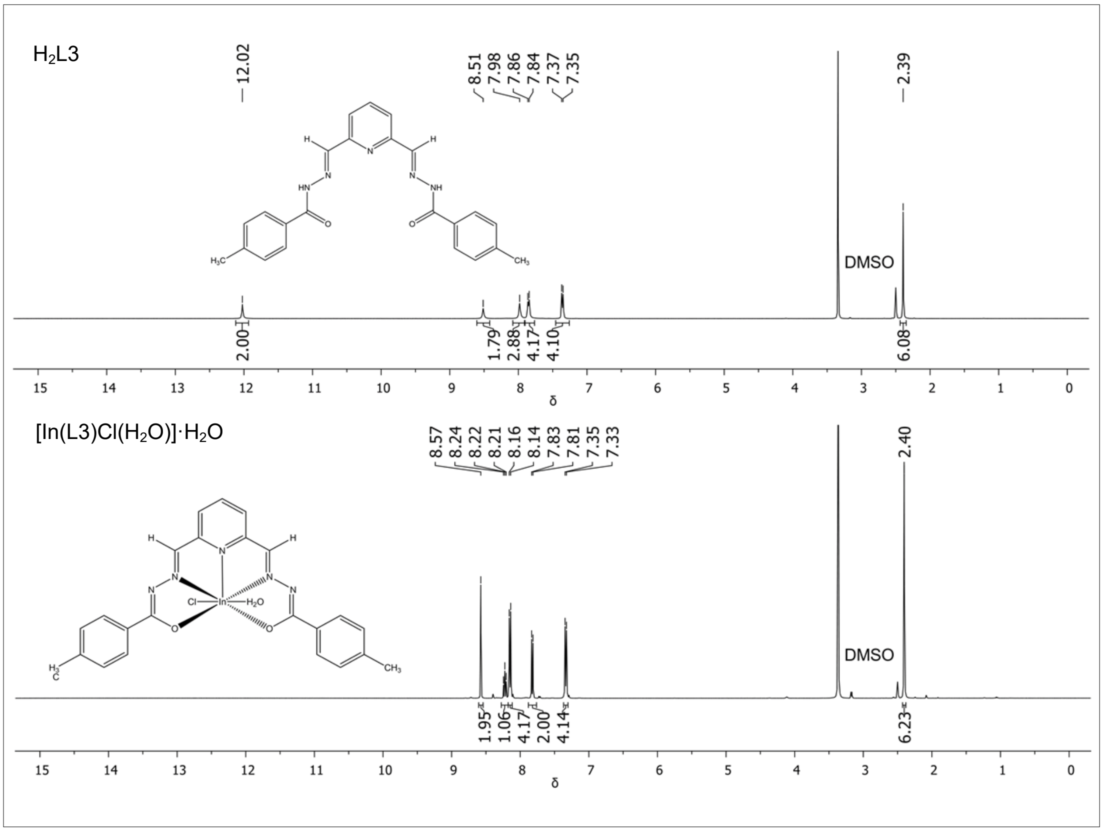

Figure S20. [1]H NMR spectra of H_2L3 and complex [In(L3)Cl(H_2O)]·H_2O (**3**)

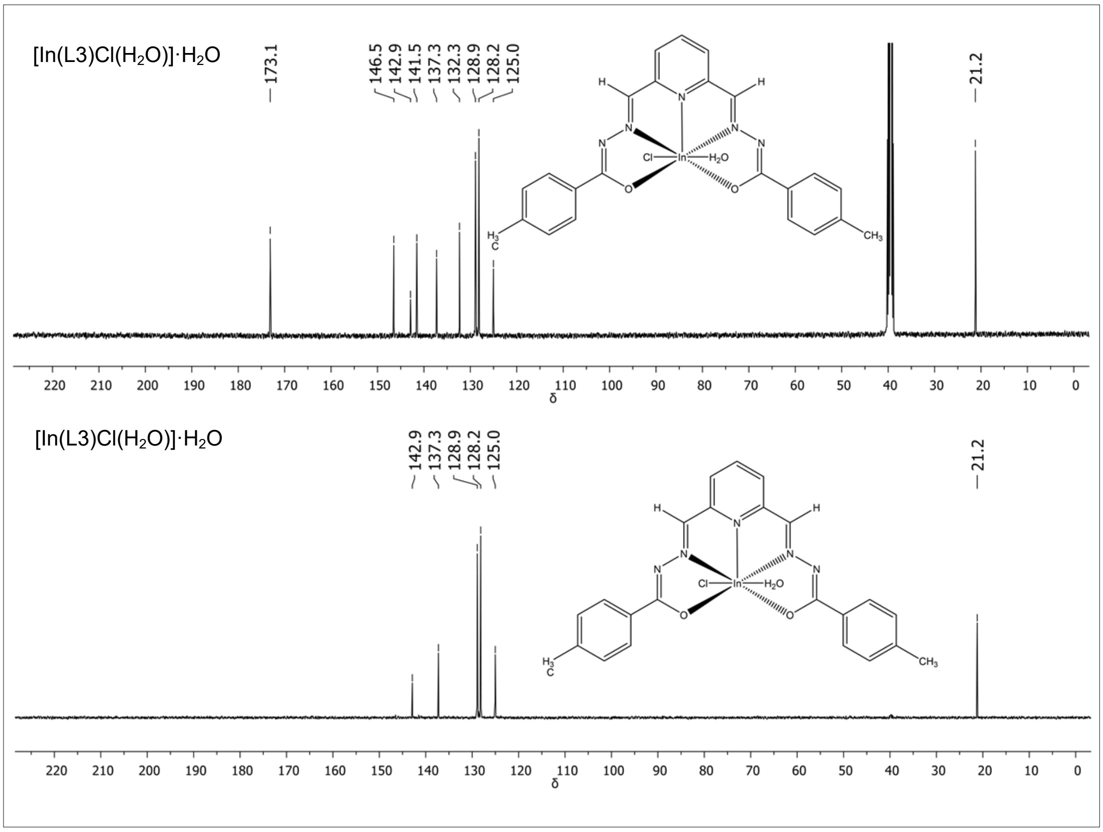

Figure S21. $^{13}C\{^{1}H\}$ and DEPT-135 NMR spectra of complex [In(L3)Cl(H_2O)]·H_2O (**3**)

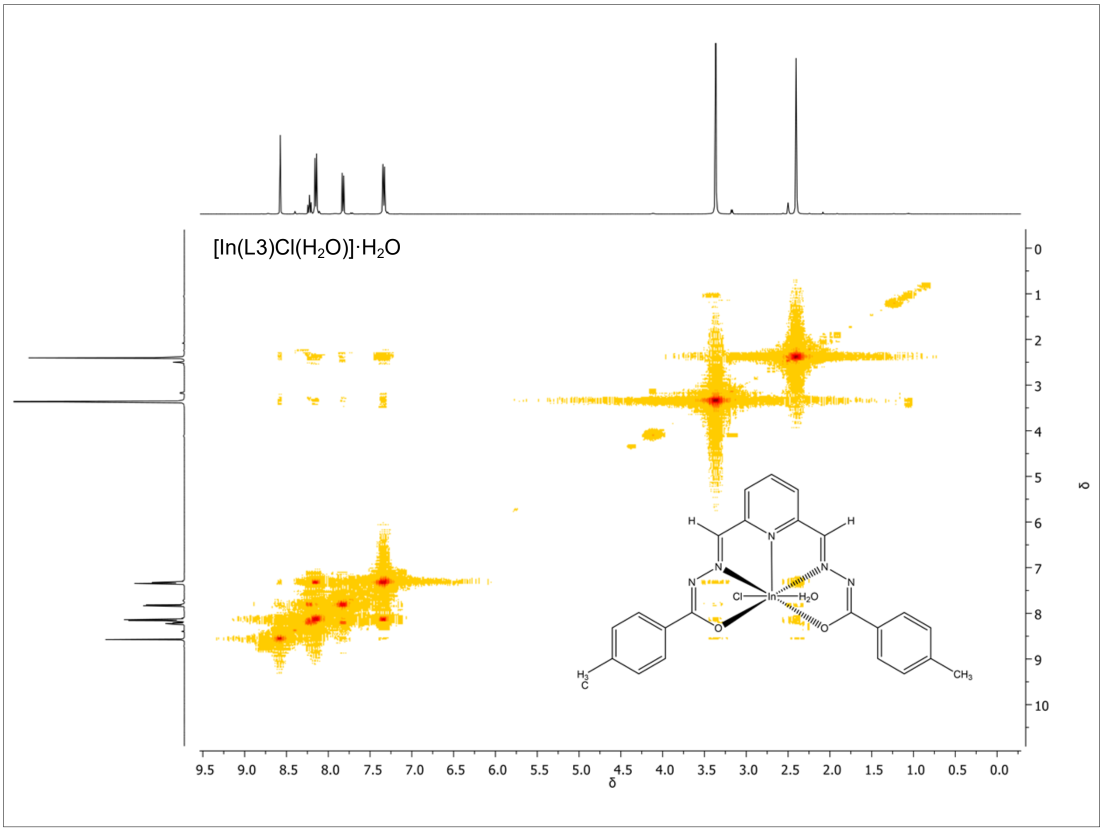

Figure S22. COSY NMR spectrum of complex [In(L3)Cl(H_2O)]·H_2O (**3**)

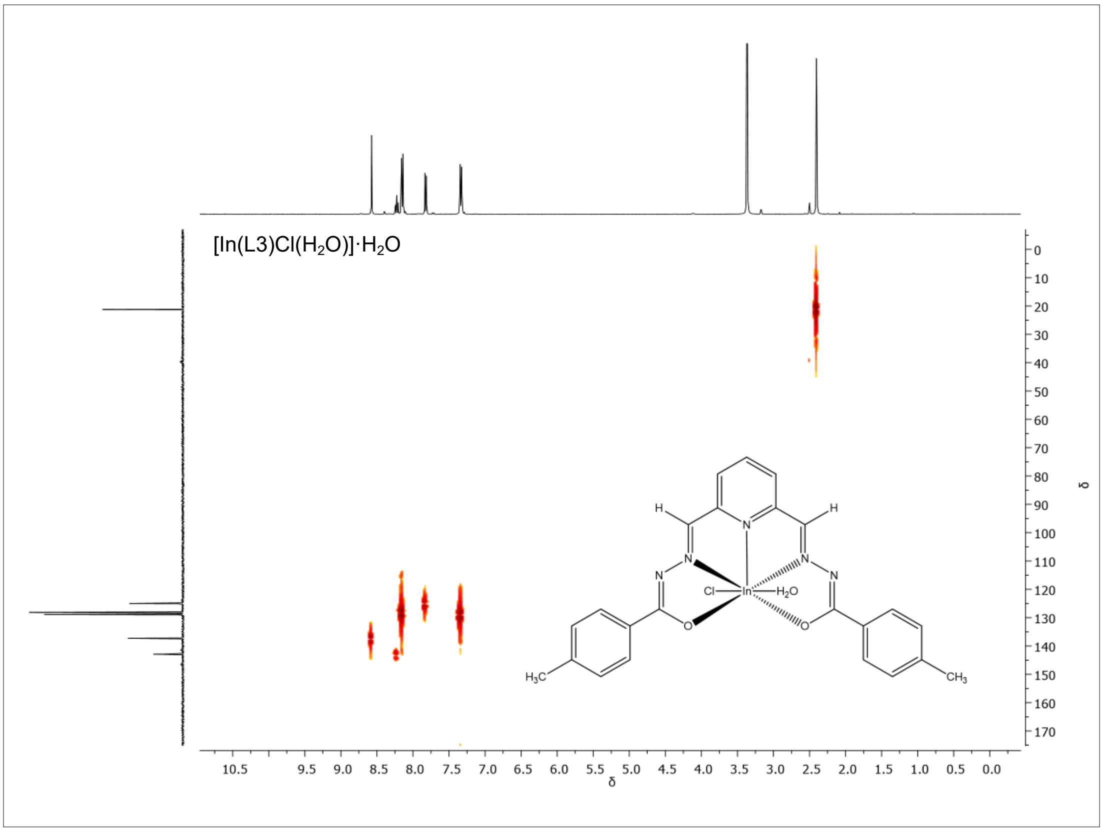

Figure S23. HMQC NMR spectrum of complex $[In(L3)Cl(H_2O)]\cdot H_2O$ (**3**)

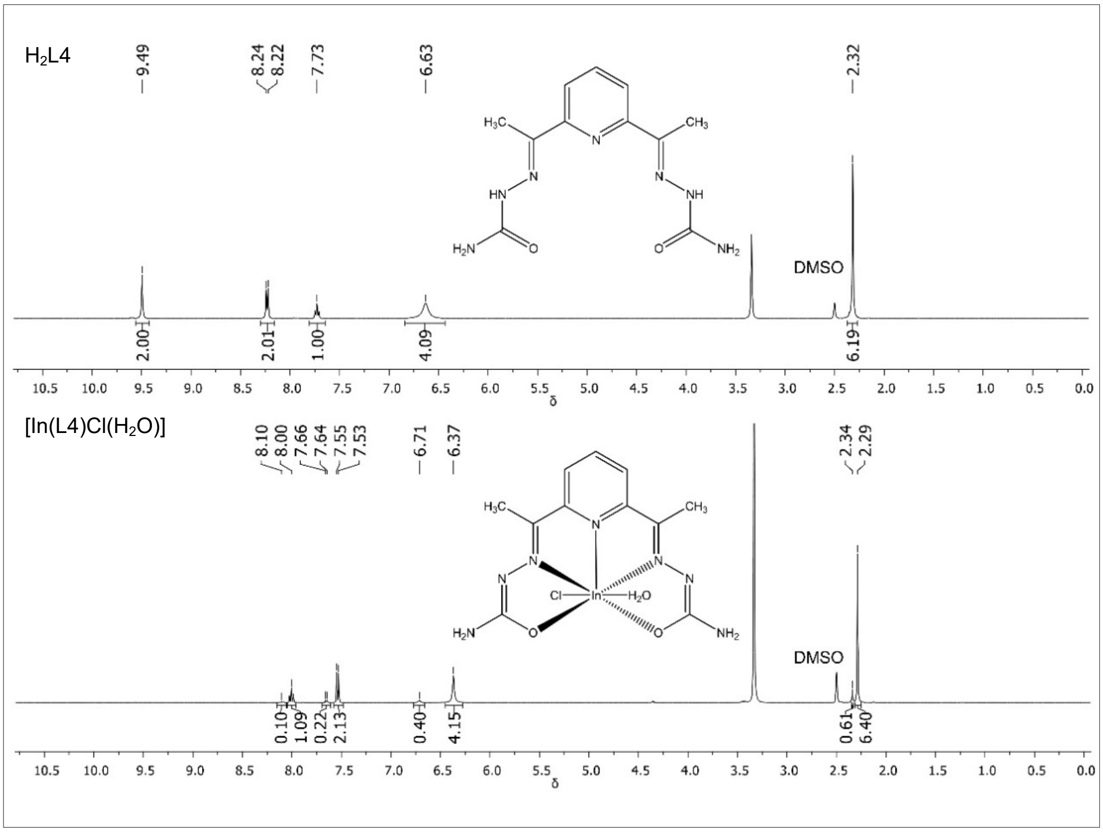

Figure S24. [1]H NMR spectra of H_2L4 and complex $[In(L4)Cl(H_2O)]$ (**4**)

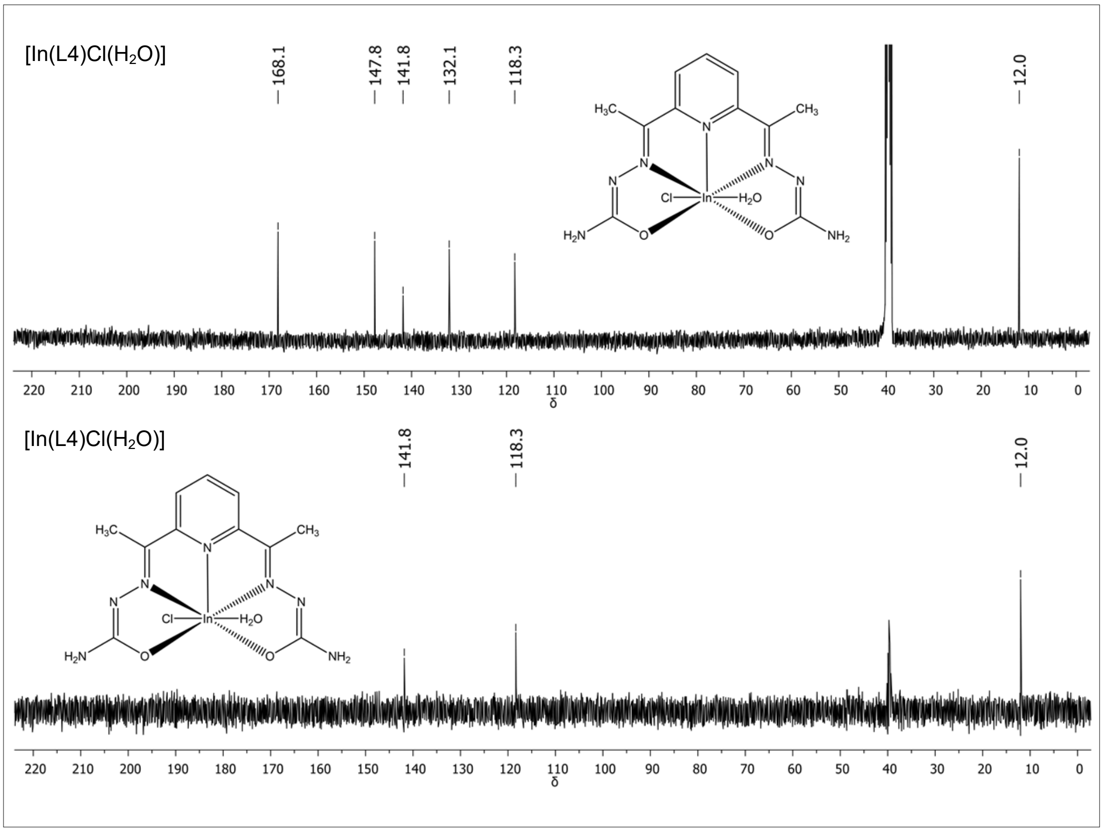

Figure S25. $^{13}C\{^{1}H\}$and DEPT-135 NMR spectra of complex [In(L4)Cl(H_2O)] (**4**)

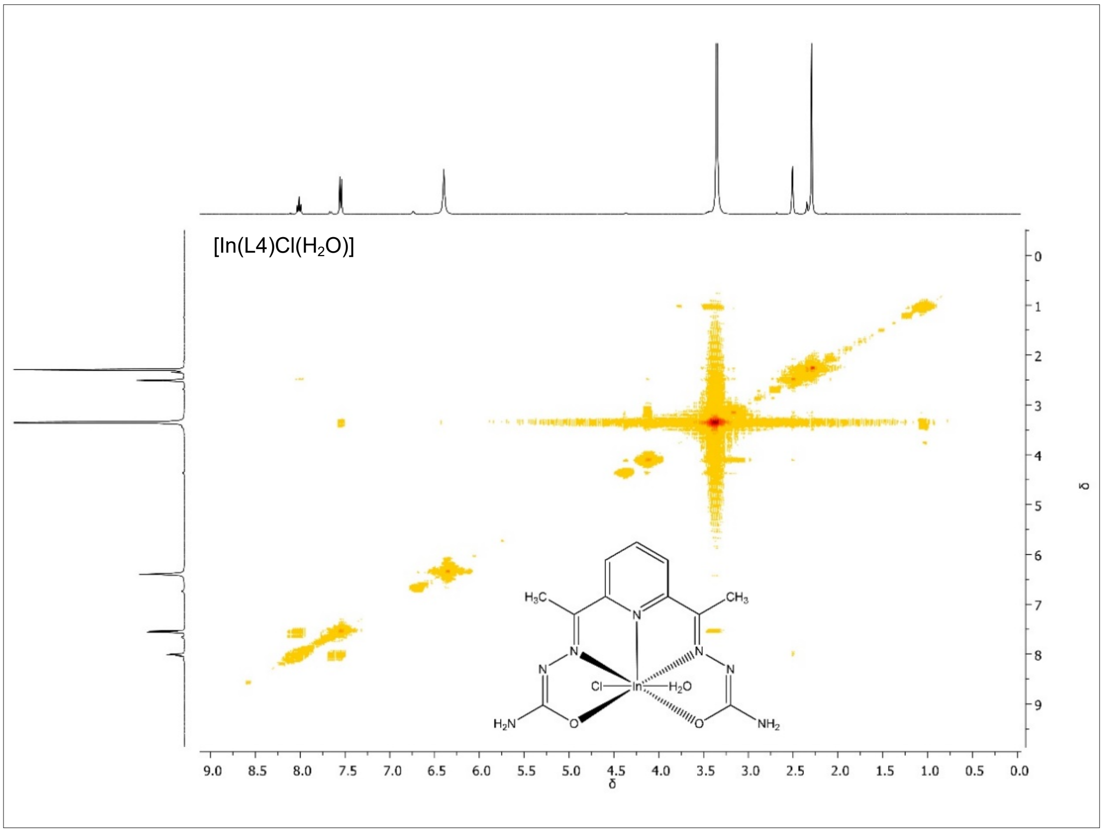

Figure S26. COSY NMR spectrum of complex [In(L4)Cl(H_2O)] (**4**)

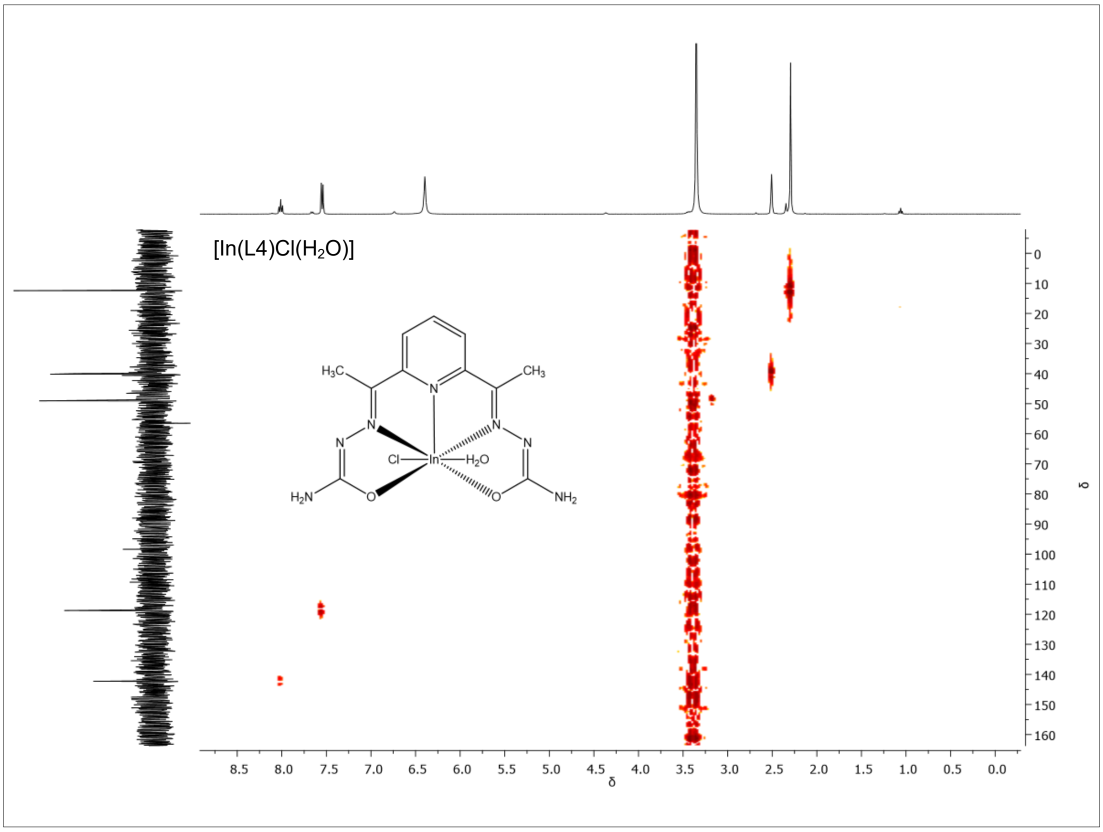

Figure S27. HMQC NMR spectrum of complex [In(L4)Cl(H_2O)] (**4**)

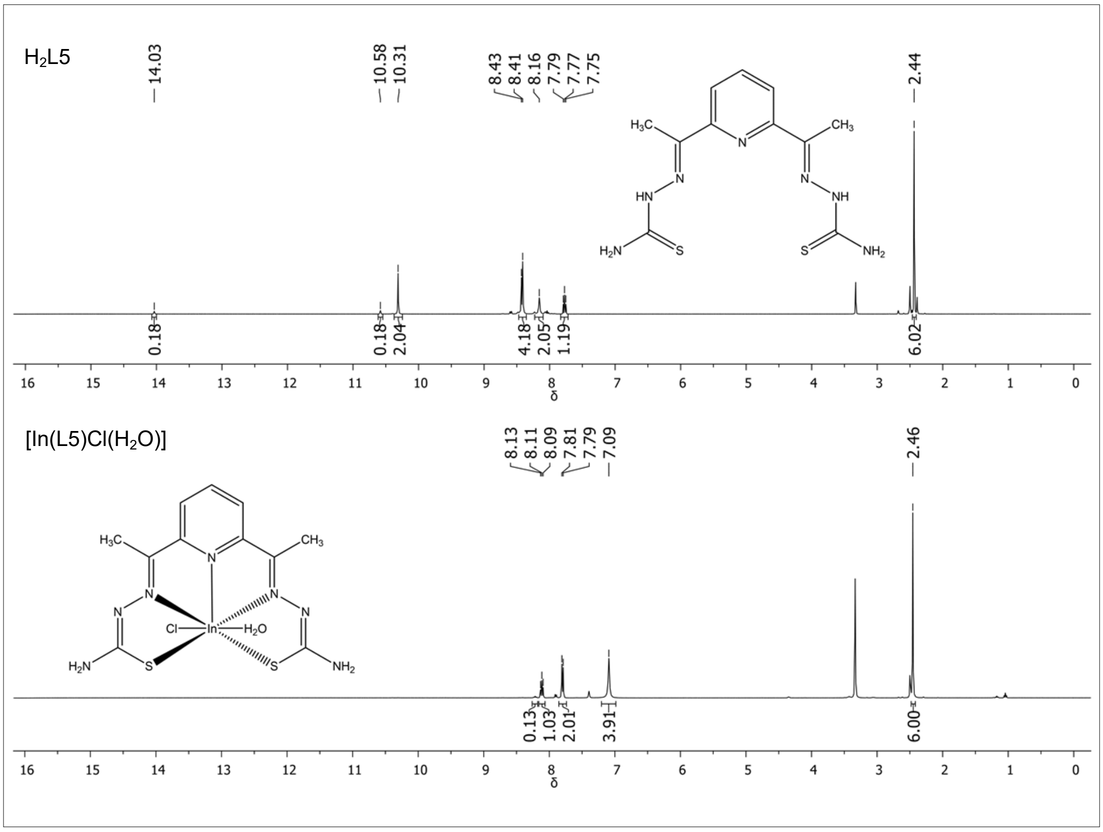

Figure S28. ^{1}H NMR spectra of H_2L5 and complex [In(L5)Cl(H_2O)] (**5**)

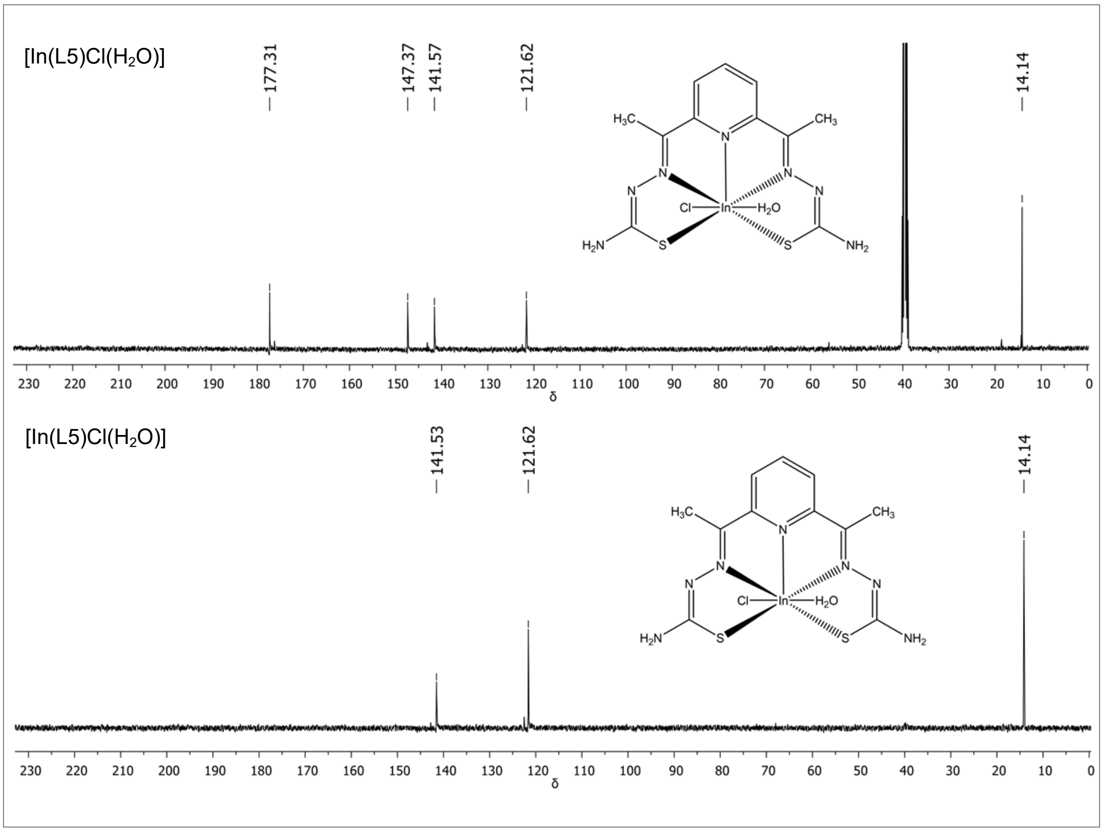

Figure S29. $^{13}C\{^{1}H\}$and DEPT-135 NMR spectra of complex [In(L5)Cl(H_2O)] (**5**)

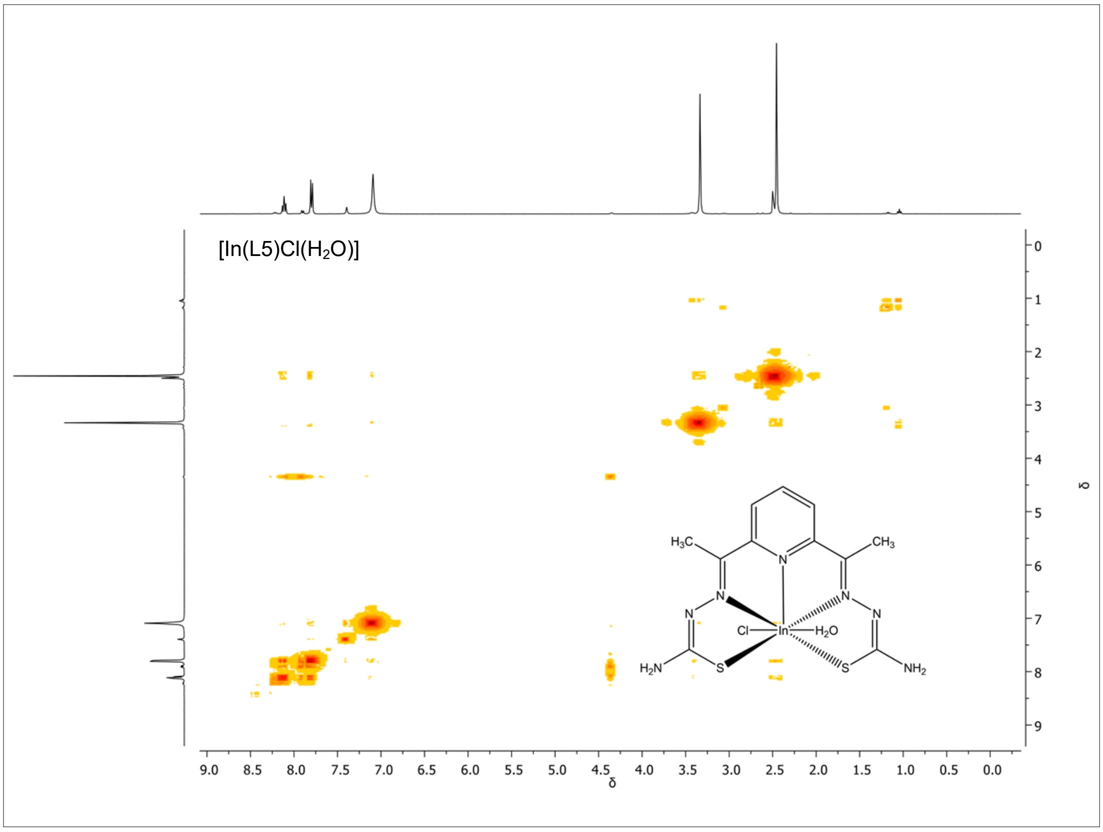

Figure S30. COSY NMR spectrum of complex [In(L5)Cl(H_2O)] (**5**)

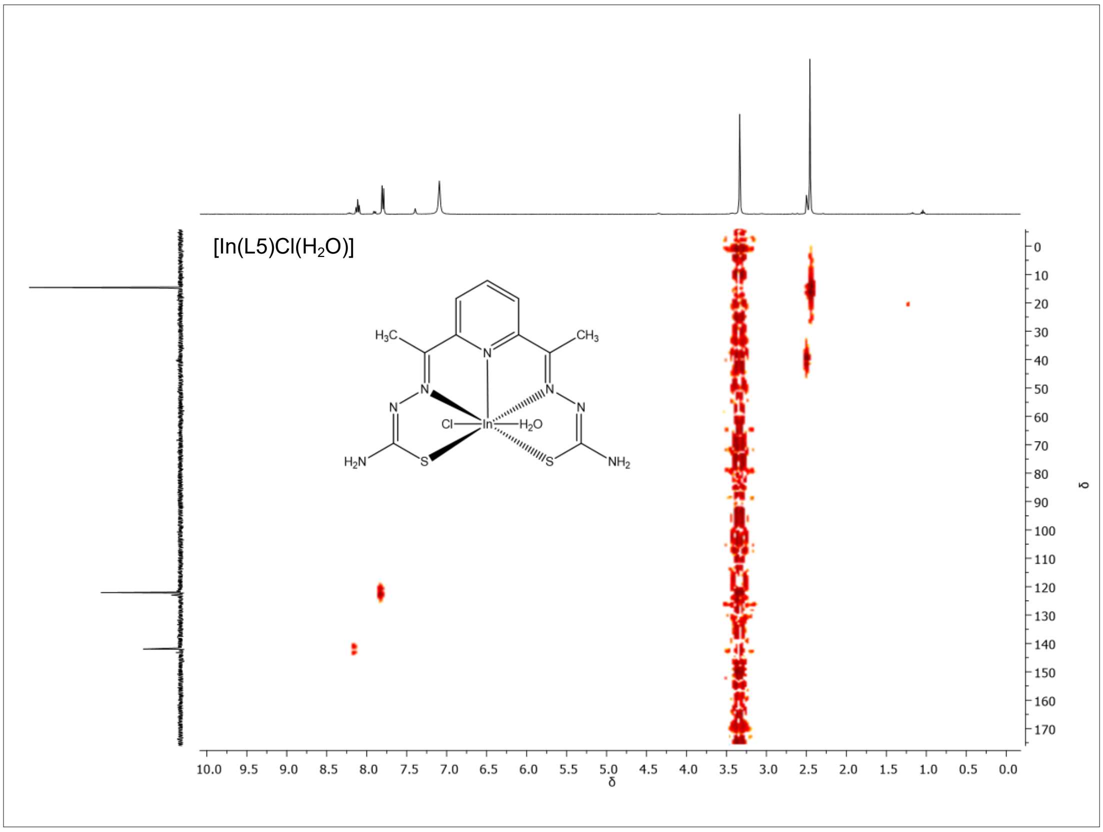

Figure S31. HMQC NMR spectrum of complex [In(L5)Cl(H_2O)] (**5**)

MALDI-TOF Mass spectra

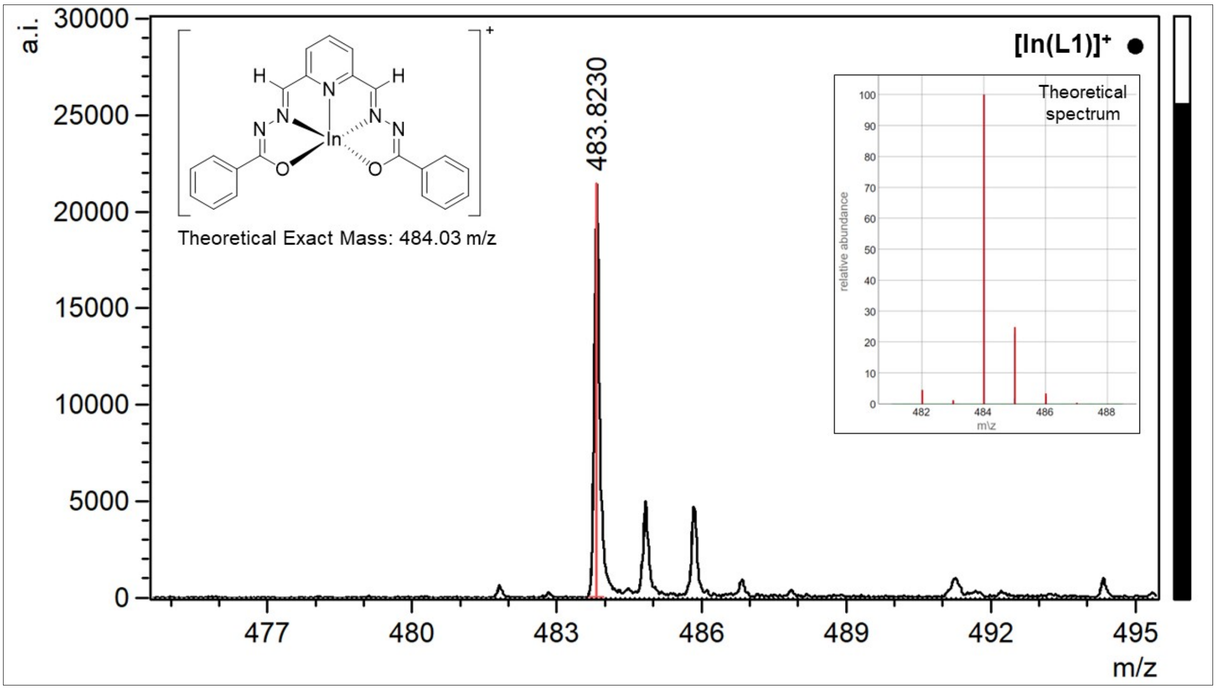

Figure S32. MALDI-TOF spectrum of complex [In(L1)Cl(H_2O)] (**1**)

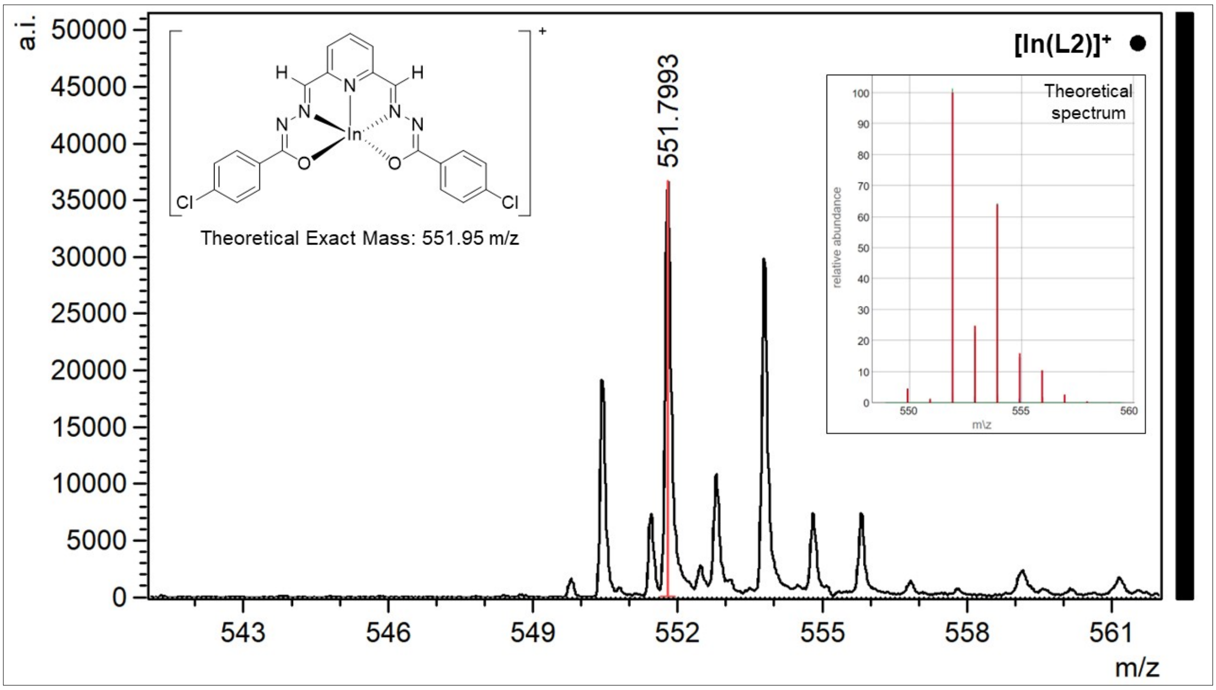

Figure S33. MALDI-TOF spectrum of complex [In(L2)Cl(H_2O)]·3H_2O (**2**)

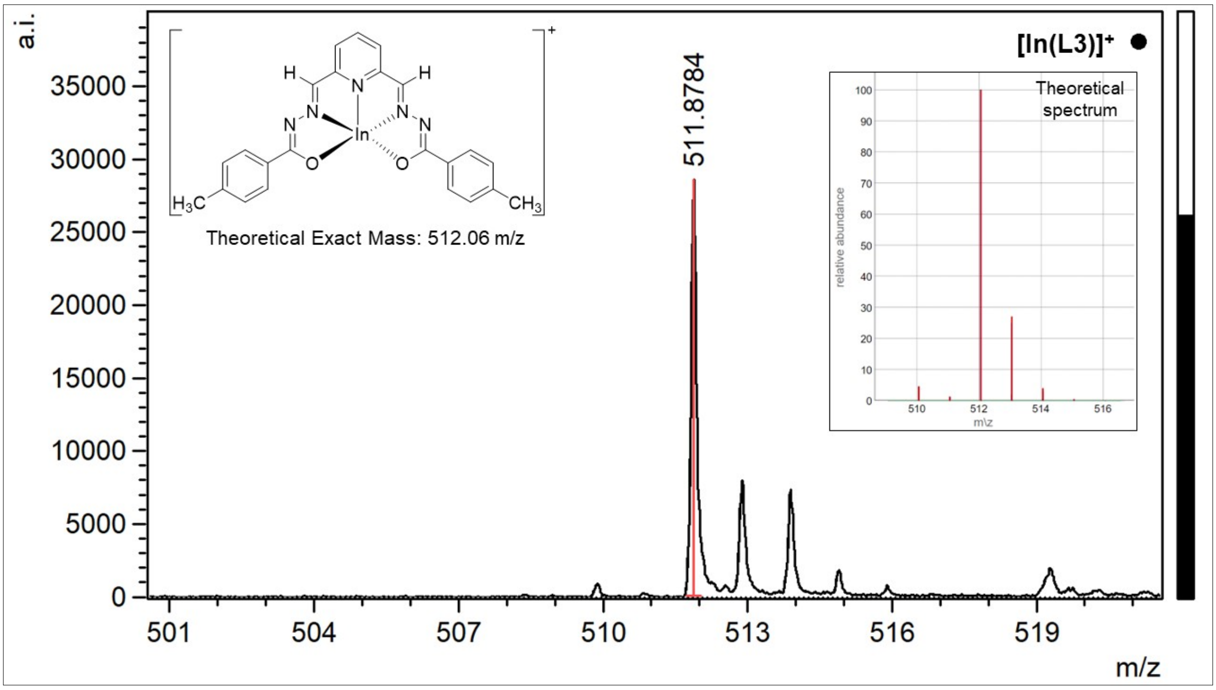

Figure S34. MALDI-TOF spectrum of complex [In(L3)Cl(H_2O)]·H_2O (**3**)

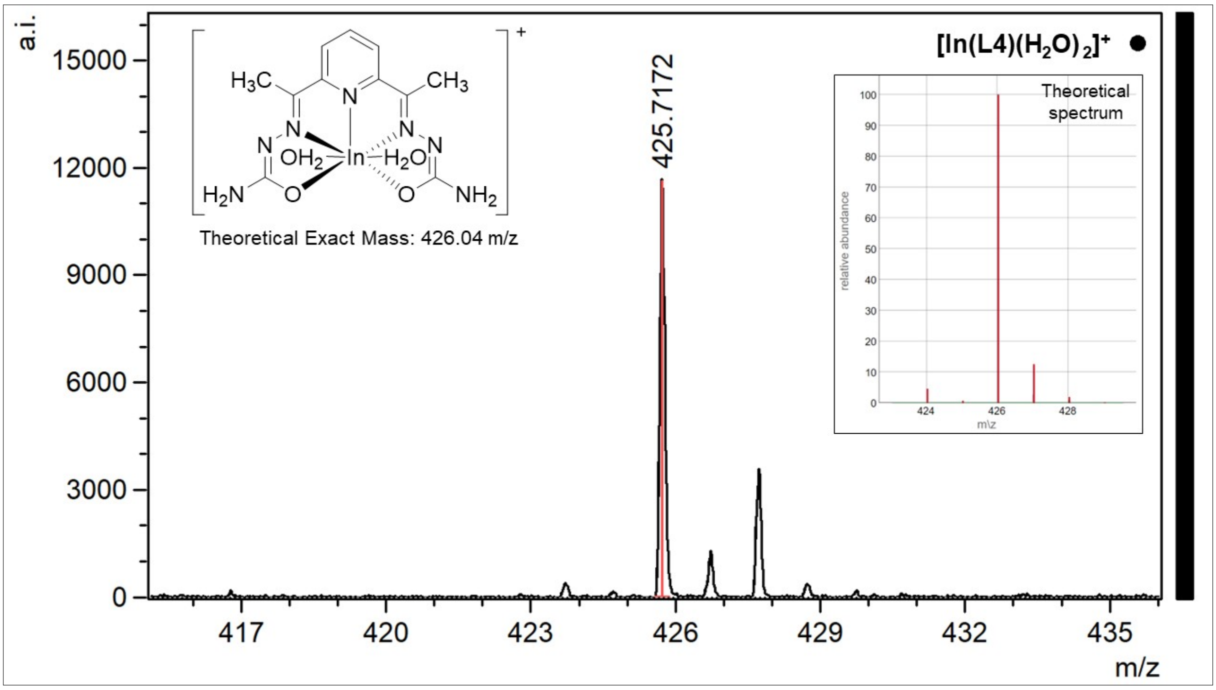

Figure S35. MALDI-TOF spectrum of complex [In(L4)Cl(H_2O)] (**4**)

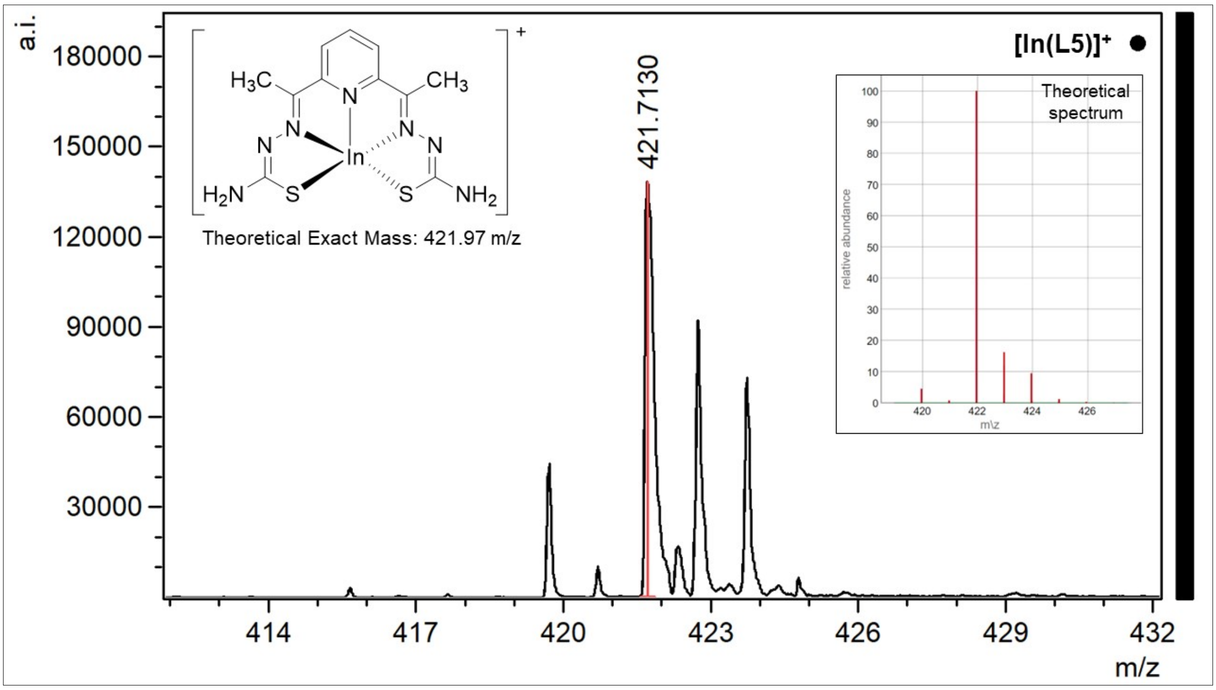

Figure S36. MALDI-TOF spectrum of complex [In(L5)Cl(H_2O)] (**5**)

Stability studies in PBS/DMSO solution

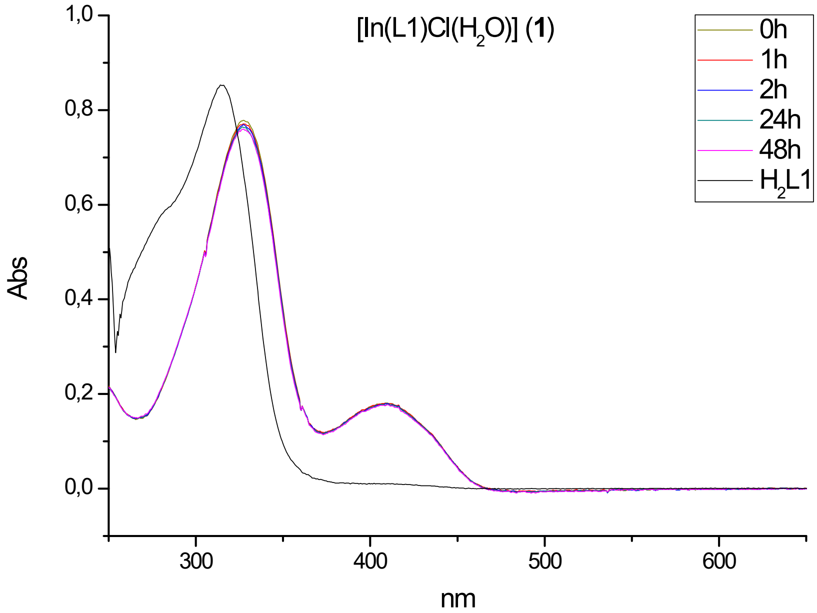

Figure S37. UV-vis absorption spectra as a function of time, of H_2L1 and complex **1** at $2x10^{-5}$ mol/L in 2% DMSO / PBS buffer, pH = 7.4.

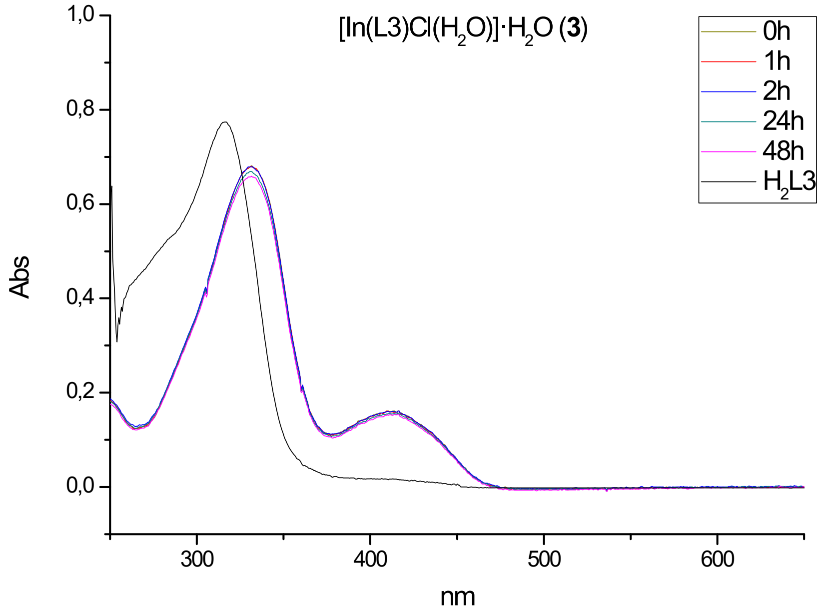

Figure S38. UV-vis absorption spectra as a function of time, of H_2L3 and complex **3** at $2x10^{-5}$ mol/L in 2% DMSO / PBS buffer, pH = 7.4.

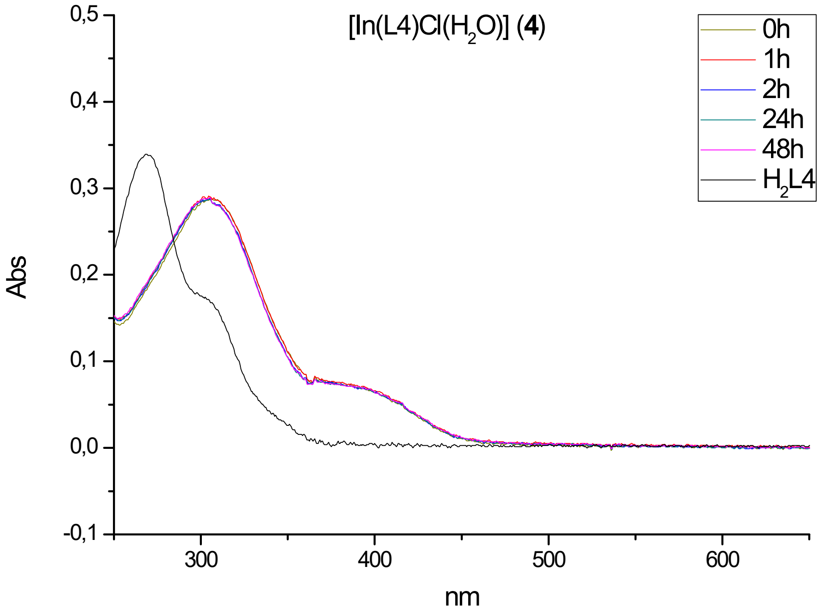

Figure S39. UV-vis absorption spectra as a function of time, of H_2L4 and complex **4** at $2x10^{-5}$ mol/L in 2% DMSO / PBS buffer, pH = 7.4.

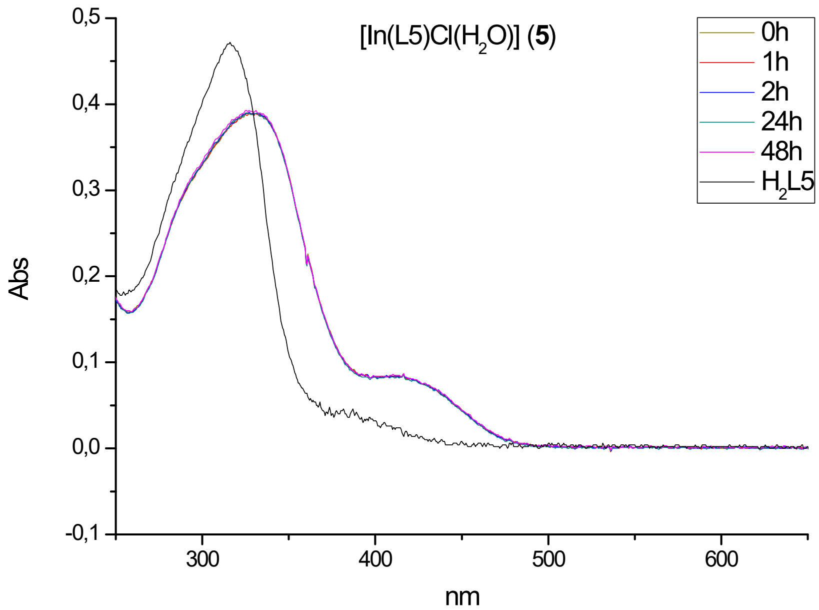

Figure S40. UV-vis absorption spectra as a function of time, of H_2L5 and complex **5** at $2x10^{-5}$ mol/L in 2% DMSO / PBS buffer, pH = 7.4.

Table S1. Comparison of radiochemotherapy, $^{114m}In(III)$ radiation monotherapy, combined In(III) chemotherapy + radiation monotherapy, in MCF-7 and MDA-MB-231 breast cancer cells.

<table>
<tr><th colspan="9">MCF-7</th></tr>
<tr><td rowspan="3">Concentration (mol/L)</td><th colspan="3">Radionuclide therapy</th><th colspan="5">Combined therapy</th></tr>
<tr><td rowspan="2">Compounds</td><td rowspan="2">Dose nGy</td><td rowspan="2">Radiochemotherapy ^{114m}In % Cell Death</td><td rowspan="2">Compounds</td><td colspan="4">Dose
% Cell Death</td></tr>
<tr><td>0 Gy</td><td>1 Gy</td><td>3 Gy</td><td>6 Gy</td></tr>
<tr><td>-</td><td>-</td><td>-</td><td>-</td><td>-</td><td>-</td><td>12.96 ± 2.87</td><td>25.84 ± 2.53</td><td>38.09 ± 3.60</td></tr>
<tr><td>10^{-6}</td><td rowspan="2">*1</td><td>0.4</td><td>40.70 ± 3.74</td><td rowspan="2">**1**</td><td>24.51 ± 2.86</td><td>34.76 ± 2.86</td><td>42.13 ± 2.52</td><td>45.12 ± 1.45</td></tr>
<tr><td>10^{-5}</td><td>4</td><td>66.35 ± 3.33</td><td>52.08 ± 2.31</td><td>62.86 ± 1.83</td><td>69.78 ± 2.26</td><td>78.16 ± 1.65</td></tr>
<tr><td>10^{-6}</td><td rowspan="2">*3</td><td>0.4</td><td>37.96 ± 3.33</td><td rowspan="2">**3**</td><td>13.62 ± 1.19</td><td>29.13 ± 1.73</td><td>40.88 ± 2.81</td><td>46.48 ± 3.49</td></tr>
<tr><td>10^{-5}</td><td>4</td><td>53.54 ± 3.49</td><td>29.78 ± 1.80</td><td>44.81 ± 2.56</td><td>56.81 ± 1.65</td><td>63.91 ± 2.79</td></tr>
<tr><td>10^{-6}</td><td rowspan="2">*4</td><td>0.4</td><td>25.20 ± 3.00</td><td rowspan="2">**4**</td><td>12.75 ± 2.19</td><td>25.80 ± 1.98</td><td>40.89 ± 1.88</td><td>53.78 ± 2.02</td></tr>
<tr><td>10^{-5}</td><td>4</td><td>40.03 ± 2.64</td><td>33.81 ± 2.50</td><td>51.70 ± 1.70</td><td>63.32 ± 1.48</td><td>66.20 ± 1.95</td></tr>
<tr><td>10^{-6}</td><td rowspan="2">*5</td><td>0.4</td><td>54.39 ± 3.09</td><td rowspan="2">**5**</td><td>25.18 ± 3.70</td><td>43.76 ± 2.80</td><td>50.47 ± 2.47</td><td>53.42 ± 2.51</td></tr>
<tr><td>10^{-5}</td><td>4</td><td>77.30 ± 3.28</td><td>54.05 ± 2.17</td><td>67.41 ± 2.13</td><td>79.63 ± 2.97</td><td>84.71 ± 3.94</td></tr>
<tr><th colspan="9">MDA-MB-231</th></tr>
<tr><td rowspan="3">Concentration (mol/L)</td><th colspan="3">Radionuclide therapy</th><th colspan="5">Combined therapy</th></tr>
<tr><td rowspan="2">Compounds</td><td rowspan="2">Dose nGy</td><td rowspan="2">Radiochemotherapy ^{114m}In % Cell Death</td><td rowspan="2">Compounds</td><td colspan="4">Dose
% Cell Death</td></tr>
<tr><td>0 Gy</td><td>1 Gy</td><td>3 Gy</td><td>6 Gy</td></tr>
<tr><td>-</td><td>-</td><td>-</td><td>-</td><td>-</td><td>-</td><td>6.69 ± 1.57</td><td>12.68 ± 1.54</td><td>20.92 ± 2.21</td></tr>
<tr><td>10^{-6}</td><td rowspan="2">*1</td><td>0.4</td><td>30.79 ± 3.47</td><td rowspan="2">**1**</td><td>19.65 ± 3.76</td><td>22.57 ± 1.63</td><td>30.99 ± 2.87</td><td>44.61 ± 3.92</td></tr>
<tr><td>10^{-5}</td><td>4</td><td>48.44 ± 2.65</td><td>37.06 ± 2.07</td><td>39.95 ± 1.91</td><td>47.50 ± 2.78</td><td>55.98 ± 4.03</td></tr>
<tr><td>10^{-6}</td><td rowspan="2">*3</td><td>0.4</td><td>26.33 ± 2.49</td><td rowspan="2">**3**</td><td>14.91 ± 3.16</td><td>18.20 ± 3.01</td><td>25.09 ± 2.44</td><td>35.92 ± 2.33</td></tr>
<tr><td>10^{-5}</td><td>4</td><td>42.99 ± 6.49</td><td>28.35 ± 2.70</td><td>33.92 ± 3.62</td><td>39.90 ± 2.10</td><td>52.01 ± 2.93</td></tr>
<tr><td>10^{-6}</td><td rowspan="2">*4</td><td>0.4</td><td>25.21 ± 3.00</td><td rowspan="2">**4**</td><td>12.75 ± 2.19</td><td>21.95 ± 2.84</td><td>24.48 ± 3.71</td><td>35.82 ± 2.99</td></tr>
<tr><td>10^{-5}</td><td>4</td><td>40.03 ± 2.64</td><td>33.81 ± 2.50</td><td>38.25 ± 1.78</td><td>44.89 ± 4.00</td><td>55.77 ± 3.09</td></tr>
<tr><td>10^{-6}</td><td rowspan="2">*5</td><td>0.4</td><td>37.78 ± 2.57</td><td rowspan="2">**5**</td><td>16.05 ± 2.85</td><td>18.11 ± 3.90</td><td>25.68 ± 1.65</td><td>36.54 ± 3.36</td></tr>
<tr><td>10^{-5}</td><td>4</td><td>59.40 ± 4.52</td><td>41.37 ± 4.16</td><td>45.14 ± 2.25</td><td>57.04 ± 1.73</td><td>63.25 ± 2.78</td></tr>
</table>